F. Marques, I. Roupa, M.T. Silva, P. Flores, H.M. Lankarani
Examination and comparison of different methods to model closed loop kinematic chains using Lagrangian formulation with cut joint, clearance joint constraint and elastic joint approaches
Mechanism and Machine Theory, 160 (2021) 104294

Examination and comparison of different methods to model closed loop kinematic chains using Lagrangian formulation with cut joint, clearance joint constraint and elastic joint approaches

Filipe Marques[1], Ivo Roupa[2], Miguel T. Silva[2], Paulo Flores[1], Hamid M. Lankarani[3]

[1] CMEMS-UMinho, Department of Mechanical Engineering, University of Minho
Campus de Azurém, 4804-533 Guimarães, Portugal
E-mail: {fmarques, pflores}@dem.uminho.pt

[2] IDMEC, Instituto Superior Técnico, Universidade de Lisboa, Lisboa, Portugal
Av. Rovisco Pais, 1, 1049-001 Lisboa, Portugal
E-mail: {ivo.roupa, MiguelSilva}@tecnico.ulisboa.pt

[3] Department of Mechanical Engineering, Wichita State University
Wichita, KS 67260-133 USA
E-mail: hamid.lankarani@wichita.edu

This paper is dedicated to Professor António Pedro Souto, who left us in December 25th, 2020

Abstract

This work aims at presenting, in a comprehensive manner, several approaches to model and simulate closed loop topologies using the classical Lagrangian formulation. One of the great advantages of the Lagrangian approach is its simplicity and easiness of obtaining the equations of motion. However, a critical aspect arises when the mechanical systems include closed loop topologies, since the process of deriving the equations of motion becomes a complex task. The key point of the present study is to convert the closed loop nature into open systems, which ultimately simplifies the modeling process when the Lagrangian formulation is utilized. For this purpose, three different methods are considered, namely those based on the cut joint approach, the clearance joint constraint model, and the elastic joint formulation are used. In the sequel of this process, a slider-crank mechanism is utilized as a demonstrative application example, and the main results are compared with those obtained with the well-established Newton-Euler method for constrained multibody systems. Moreover, this example allows the comparison of the main characteristics and peculiarities of the described approaches.

Keywords: Newton-Euler Method, Lagrangian Formulation, Closed Loop Kinematic Chains, Open Systems, Multibody System Dynamics

1. Introduction

Over the last few decades, there has been an increasing interest in the development of the equations of motion for multibody systems, that is, systems with multiple bodies whose interactions are affected by the application of external forces and by the presence of kinematic joints or constraints. The main reason for that is because many complex systems, such as mechanisms, manipulators, biosystems, etc., can be modeled and analyzed with a multibody system approach. By and large, the process of deriving the equations of motion for constrained multibody systems has been developed over the last decades along with two fundamental approaches, namely the vectorial mechanics and the analytical mechanics. In the vectorial method, which is supported by Newton-Euler's laws of motion of rigid bodies using Cartesian coordinates and kinematic constraints, the dynamics of the systems is evaluated taking into account vectorial quantities, chiefly force and momentum [1, 2]. In turn, in analytical or variational mechanics approach, which is based on the Lagrange's equations of motion, two scalar quantities play a key role in the process of modeling multibody systems, namely mechanical

energy and work [3]. In fact, these are the two most popular and frequent formulations, when dealing with dynamic modeling and analysis of constrained multibody systems in which the bodies experience large displacements [4-10]. Aside from these two fundamental formulations, there are several other methodologies available in the literature to derive the equations of motion for constrained multibody systems, each having their own peculiarities and field of application. Amongst the various alternative formulations to develop the equations of motion, those proposed by d'Alembert [11], Hamilton [12], Maggi [13], Gibbs-Appell [14, 15], Jourdain [16], Kane [17-19], Dirac [20], Hooker and Margulies [21], Pars [22], Udwadia-Kalaba [23], should be mentioned here. These several formulations of constrained multibody systems dynamics can differ in the principle considered, type of coordinates adopted, and methods used to handle the violation of constraints [24-31]. Schiehlen [32] has described dozens of different formulations that allow for the generation of the equations of motion.

One of the major differences between Newton-Euler and Lagrangian formulations comes from the type of coordinates adopted to define the geometric configuration of the system under analysis. Thus, the Newton-Euler equations of motion are typically derived using absolute coordinates, that is a set of Cartesian and angular coordinates, to characterize the configuration of each body with respect to an inertial reference frame [5, 6]. This choice of coordinates implies the use of constraint equations with the purpose of establishing the kinematic relations between adjacent and constrained bodies. The consideration of absolute coordinates allows for the systematic generation of the equations of motion, in the measure that each body has the similar representation and, hence, the kinematic constraint equations can be easily obtained [33]. This feature is of paramount importance when a general-purpose code is required. A drawback associated with absolute coordinates is the large number of equations, which eventually leads to inefficient construction and resolution of the equations of motion. In turn, the Lagrangian method is developed on the basis of generalized coordinates, which have the advantage of leading to a smaller number of equations. Additionally, the use of generalized coordinates does not require for algebraic constraint equations [34]. For open loop kinematic chains, the generalized coordinates are independent coordinates, while for closed loop chains, a minimum number of independent coordinates must be established. In general, this option leads to efficient resolution of the equations of motion in terms of coordinates, mainly when dealing with open loop systems. However, the generation of the equations of motion with generalized coordinates can exhibit a high level of nonlinearity for closed systems, in the measure that they are quite difficult to derive. This feature limits their implementation in general computer codes. It is worth to mention that there are several alternative types of coordinates that can be used to derive the equations of motion for multibody systems, and the interested reader on the details is referred to references [35-44].

The Newton-Euler method constitutes a quite attractive approach to generate the equations of motion for constrained multibody mechanical systems, because it is a direct and straightforward formulation, and a very interesting choice for developing general-purpose codes. In a simple manner, the Newton-Euler method provides a collection of differential equations for the bodies, together with a set of algebraic constraint equations that represents the kinematic pairs, resulting in the equations of motion to be a system of differential algebraic equations (DAE) [45]. To promote the easiness of resolution of the equations of motion, the kinematic constraint equations are differentiated to include the accelerations constraint equations directly into the equations of motion to achieve a set of ordinary differential equations (ODE). In general, this formulation leads to solutions with a large number of equations, but with a low level of complexity and nonlinearity. The Newton-Euler approach uses absolute coordinates and, consequently, a high number of coordinates and kinematic constraints are required, reason why this method is often named as maximal coordinates formulation. A drawback associated with the Newton-Euler method is the necessity to incorporate an effective technique to handle the violation of constraints, such as the well-established Baumgarte method [46], since the kinematic constraints are not directly included in the equations of motion. Thus, the Newton-Euler approach is typically not appropriate for the dynamics and control of complex systems due to the large number of different states. As mentioned earlier, this approach can be used with diverse types of coordinates, resulting

in different formulation, such as body-coordinates, point-coordinates and joint-coordinates, having each one of them specific advantages and disadvantages for a certain case of study [47].

The Lagrangian formulation can be a quite useful alternative to Newton-Euler method to apply to mechanical systems with large number of bodies, in particular when the systems have open kinematic structures. In a simple manner, the Lagrangian formulation provides a set of ODE and does not require the incorporation of kinematic constraint equations, since they are implicitly taken into consideration. Therefore, the obtained solutions do not need any method to eliminate or minimize the violation of constraints, making the computational resolution of the equations of motion a quite efficient process in dynamics and control of simple systems [34]. The Lagrangian formulation results in a small number of equations of motion, because it uses generalized coordinates in the process of their derivation. In most of the cases, the number of equations of motion is equal to system's degrees-of-freedom, reason why this methodology is often named as minimal coordinates formulation [48]. The equations of motion derived with the Lagrangian method can exhibit terms with high degree of complexity and nonlinearity. This issue is particularly critical when dealing with mechanical systems with closed loop topologies, such as in mechanisms and parallel manipulators [49, 50]. This feature can be considered as a drawback in terms of systematization and implementation in computer codes. In addition, the final form of the equation of motion is, in general, quite difficult to analyze and interpret from a physical point of view, in the measure that generalized variables are considered in the process of the generation of the equations of motion.

It must be highlighted that the problem of dynamic modeling and simulation of multibody mechanical systems that include closed loop topologies is a nontrivial task when the Lagrangian formulation is to be employed. This methodology requires a significant amount of mathematical complex manipulation in order to obtain the necessary derivatives to generate the Lagrange's equations of motion. A reason for that deals with the closed loop nature of the systems, which implies the use of a very few number of degrees-of-freedom, and, therefore, the number of generalized independent coordinates is quite small too. Hence, the center of mass coordinates and velocities, which need to be expressed in terms of generalized independent coordinates, reveal complex and nonlinear relations that affect the mathematical issues described above. In sharp contrast, the Newton-Euler method does not require any derivatives, because it is based on a direct and standard procedure that can be applied to all of the bodies that belong to a mechanical system, independently of the having open and/or closed kinematic chains.

Thus, the main focus of this work is to examine and compare several different formulations to model constrained multibody systems with closed loop topologies based on the classical Lagrangian method. For this purpose, three approaches are presented, for which the fundamental feature is to transform the closed loop kinematic chains into open ones, in order to facilitate the application of the Lagrangian formulation. The three methodologies described in the following sections are based on the cut joint approach, the clearance joint method and the elastic joint formulation available in the literature. The cut joint approach is based on the use of Lagrange multipliers associated with the vector loop closure constraints in the dynamics equations of motion. The clearance joint approach utilizes a single Lagrange multiplier for a distance or virtual link constraint. The elastic joint approach treats the system as open loop with resistive elastic springs replaced at the cut joint. These approaches allow the use of suitable alternatives for the utilization of the Lagrangian formulation into closed loop systems by closing them recurring to distinct kinematic and force constraints. In the sequel of this process, the academic planar slider-crank mechanism with ideal joints is considered with the objective of demonstrating the particular characteristics and potential limitations related to each methodology described, namely in terms of computational accuracy and efficiency.

The remaining of this paper is organized as follows. In section 2, the Newton-Euler method is revised and applied to a planar slider-crank mechanism, which is of interest for the aim of this study and constitutes the reference of comparison for other approaches considered. A detailed analysis of the Lagrangian formulation is presented in section 3, where the slider-crank system is also utilized, since it includes a closed loop kinematic chain. Then, Sections 4, 5, and 6 deal with

the Lagrangian formulations with cut joints, clearance joints and elastic joints, respectively, and the slider-crank mechanism is again utilized. In section 7, a collection of the results obtained from computational simulations of the proposed approaches are presented and discussed. A summary of this study and concluding remarks are provided in section 8.

2. Newton-Euler formulation with absolute or cartesian coordinates

The Newton-Euler approach is among the most popular methods to formulate the equations of motion for dynamic modeling and analysis of multibody mechanical systems [51]. This formulation is simple, direct and quite intuitive for general-purpose codes to model multibody systems. Thus, this section is aimed at presenting, in a review manner, the key ingredients related to Newton-Euler formulation. For that, the academic slider-crank mechanism is selected as a demonstrative application example. Figure 1 shows a generic configuration of the planar slider-crank system, which consists of three rigid moving bodies, namely the crank (1), the connecting rod (2) and the slider (3). The ground is the fixed body and it is numbered as 0. Three revolute joints and one translational joint impose a total of eight kinematic constraints. The Newton-Euler formulation can be developed using absolute center of mass coordinates, reason this approach is often referred to as body-coordinate formulation [52]. Thus, the vector of coordinates that completely describes the configuration of the slider-crank multibody model is expressed as [53]

$$\mathbf{c} = \left\{ x_1 \quad y_1 \quad \theta_1 \quad x_2 \quad y_2 \quad \theta_2 \quad x_3 \quad y_3 \quad \theta_3 \right\}^{\mathrm{T}} \tag{1}$$

in which **c** is a 9×1 vector that includes two Cartesian coordinates and one angle, with respect to a global system, per body. The nine absolute coordinates in Eq. (1) are not independent, since the slider-crank mechanism has one degree-of-freedom. This results from three moving bodies and eight non-redundant constraints that represent the kinematic restrictions associated with revolute and translational joints [54].

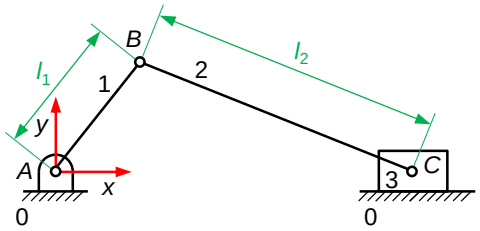

Fig. 1. Generic configuration of the planar slider-crank mechanism.

For the dynamic analysis, the slider-crank mechanism is initialized with the crank angular velocity equal to 150 rad/s. At the start of the dynamic simulations of the slider-crank multibody model, the crank and connecting rod are aligned in the *x* direction, which corresponds to the top dead point. The geometric and inertia properties of each body of the slider-crank mechanism are listed in Table 1.

Table 1. Geometric and inertia properties for the slider-crank mechanism.

Body	Length [m]	Mass [kg]	Moment of inertia [kg·m^2]
Crank (1)	0.153	0.038	7.4×10^{-5}
Connecting rod (2)	0.306	0.076	5.9×10^{-5}
Slider (3)	-	0.038	1.8×10^{-6}

In order to be able to construct the equations of motion for the slider-crank mechanism based on the Newton-Euler formulation, it is first necessary to draw the free-body diagrams of each system component, as shown in Fig. 2. For the sake of simplicity, the centers of mass of the crank and connecting rod are located at the midpoint of the corresponding bodies, while the center of mass of the slider is positioned at the revolute joint *C*. The Newton's third law is considered in the representation of the free-body diagrams, namely in what concerns the joint reactions [55]. The free-body diagrams allow for a simple and clear description of all the applied and reaction forces and moments that act on each body of the slider-crank mechanism. Moreover, the gravitational forces are the only external applied forces considered in the present study.

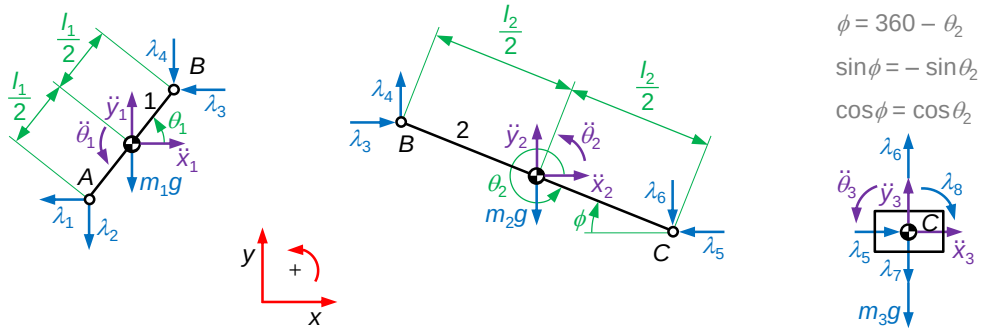

Fig. 2. Free-body diagrams of each body of the slider-crank mechanism.

With regard to Fig. 2, the seven reaction forces and one reaction moment at the kinematic joints of this multibody system can be condensed in an 8×1 vector in the form

$$\boldsymbol{\lambda} = \begin{Bmatrix} \lambda_1 & \lambda_2 & \lambda_3 & \lambda_4 & \lambda_5 & \lambda_6 & \lambda_7 & \lambda_8 \end{Bmatrix}^{\mathrm{T}} \tag{2}$$

The Newton-Euler equations of motion of the slider-crank mechanism can be constructed with regard to the free-body diagrams depicted in Fig. 2, resulting in a total of nine translational and rotational equations as

$$m_1\ddot{x}_1 = -\lambda_1 - \lambda_3 \tag{3}$$

$$m_1\ddot{y}_1 = -\lambda_2 - \lambda_4 - m_1 g \tag{4}$$

$$I_1\ddot{\theta}_1 = -\lambda_1 \frac{l_1}{2}\sin\theta_1 + \lambda_2 \frac{l_1}{2}\cos\theta_1 + \lambda_3 \frac{l_1}{2}\sin\theta_1 - \lambda_4 \frac{l_1}{2}\cos\theta_1 \tag{5}$$

$$m_2\ddot{x}_2 = \lambda_3 - \lambda_5 \tag{6}$$

$$m_2\ddot{y}_2 = \lambda_4 - \lambda_6 - m_2 g \tag{7}$$

$$I_2\ddot{\theta}_2 = \lambda_3 \frac{l_2}{2}\sin\theta_2 - \lambda_4 \frac{l_2}{2}\cos\theta_2 + \lambda_5 \frac{l_2}{2}\sin\theta_2 - \lambda_6 \frac{l_2}{2}\cos\theta_2 \tag{8}$$

$$m_3\ddot{x}_3 = \lambda_5 \tag{9}$$

$$m_3\ddot{y}_3 = \lambda_6 - \lambda_7 - m_3 g \tag{10}$$

$$I_3\ddot{\theta}_3 = -\lambda_8 \tag{11}$$

This set of equations represents the Newton-Euler, or translational and rotational, equations of motion of the slider-crank mechanism, which constitutes a linear system of nine equations with 17 unknowns, namely nine accelerations and eight joint reactions. Equations (3)-(11) can be rewritten in a compact form as [53]

$$\mathbf{M}\ddot{\mathbf{c}} = \mathbf{h}_{\mathrm{a}} + \mathbf{h}_{\mathrm{r}} \tag{12}$$

where $\mathbf{M}$ is a 9×9 constant and diagonal mass or inertia matrix that contains the masses and mass moments of inertia of the bodies, $\ddot{\mathbf{c}}$ is a 9×1 vector of linear and rotational accelerations, $\mathbf{h}_{\mathrm{a}}$ denotes a 9×1 vector of applied forces and moments, and $\mathbf{h}_{\mathrm{r}}$ represents a 9×1 vector that includes joint reaction forces and moments. This set of arrays can be expressed as

$$\mathbf{M} = \mathrm{diag}\begin{bmatrix} m_1 & m_1 & I_1 & m_2 & m_2 & I_2 & m_3 & m_3 & I_3 \end{bmatrix} \tag{13}$$

$$\ddot{\mathbf{c}} = \begin{Bmatrix} \ddot{x}_1 & \ddot{y}_1 & \ddot{\theta}_1 & \ddot{x}_2 & \ddot{y}_2 & \ddot{\theta}_2 & \ddot{x}_3 & \ddot{y}_3 & \ddot{\theta}_3 \end{Bmatrix}^{\mathrm{T}} \tag{14}$$

$$\mathbf{h}_{\mathrm{a}} = \begin{Bmatrix} 0 & -m_1 g & 0 & 0 & -m_2 g & 0 & 0 & -m_3 g & 0 \end{Bmatrix}^{\mathrm{T}} \tag{15}$$

$$\mathbf{h}_{\mathrm{r}} = -\begin{bmatrix} 1 & 0 & 1 & 0 & 0 & 0 & 0 & 0 \\ 0 & 1 & 0 & 1 & 0 & 0 & 0 & 0 \\ \frac{l_1}{2}\sin\theta_1 & -\frac{l_1}{2}\cos\theta_1 & -\frac{l_1}{2}\sin\theta_1 & \frac{l_1}{2}\cos\theta_1 & 0 & 0 & 0 & 0 \\ 0 & 0 & -1 & 0 & 1 & 0 & 0 & 0 \\ 0 & 0 & 0 & -1 & 0 & 1 & 0 & 0 \\ 0 & 0 & -\frac{l_2}{2}\sin\theta_2 & \frac{l_2}{2}\cos\theta_2 & -\frac{l_2}{2}\sin\theta_2 & \frac{l_2}{2}\cos\theta_2 & 0 & 0 \\ 0 & 0 & 0 & 0 & -1 & 0 & 0 & 0 \\ 0 & 0 & 0 & 0 & 0 & -1 & 1 & 0 \\ 0 & 0 & 0 & 0 & 0 & 0 & 0 & 1 \end{bmatrix} \begin{Bmatrix} \lambda_1 \\ \lambda_2 \\ \lambda_3 \\ \lambda_4 \\ \lambda_5 \\ \lambda_6 \\ \lambda_7 \\ \lambda_8 \end{Bmatrix} \tag{16}$$

The vector of joint reaction forces is expressed as a coefficient matrix times the vector of the components of reaction forces and moments, that is, the vector of Lagrange multipliers given by Eq. (2). Indeed, the coefficient matrix represents the directions of the reaction forces and moment arms, or levers, of the reaction moments [56].

Thus, in order to ensure that the multibody model has a unique and appropriate solution, it is necessary to take into account eight additional equations that result from kinematic constraints associated with the revolute and translational joints. Thus, with regard to Fig. 1, eight algebraic constraint equations can be easily obtained as

$$\Phi_1 \equiv x_1 - \frac{l_1}{2}\cos\theta_1 = 0 \tag{17}$$

$$\Phi_2 \equiv y_1 - \frac{l_1}{2}\sin\theta_1 = 0 \tag{18}$$

$$\Phi_3 \equiv x_1 + \frac{l_1}{2}\cos\theta_1 - x_2 + \frac{l_2}{2}\cos\theta_2 = 0 \tag{19}$$

$$\Phi_4 \equiv y_1 + \frac{l_1}{2}\sin\theta_1 - y_2 + \frac{l_2}{2}\sin\theta_2 = 0 \tag{20}$$

$$\Phi_5 \equiv x_2 + \frac{l_2}{2}\cos\theta_2 - x_3 = 0 \tag{21}$$

$$\Phi_6 \equiv y_2 + \frac{l_2}{2}\sin\theta_2 - y_3 = 0 \tag{22}$$

$$\Phi_7 \equiv y_3 = 0 \tag{23}$$

$$\Phi_8 \equiv \theta_3 = 0 \tag{24}$$

The set of algebraic constraint equations (17)-(24) can be expressed in a generic and compact form as [53]

$$\boldsymbol{\Phi} \equiv \boldsymbol{\Phi}(\mathbf{c}) = \mathbf{0} \tag{25}$$

The constraint equations (25) are developed at the position level, and therefore, they cannot be directly appended to equations of motion (12), but the constraint equations at the acceleration level must be considered instead. Thus, the first time derivative of Eq. (25) yields the constraint equations at the velocity level, which can be written as

$$\dot{\boldsymbol{\Phi}} \equiv \mathbf{D}\dot{\mathbf{c}} = \mathbf{0} \tag{26}$$

in which $\mathbf{D}$ denotes an 8×9 Jacobian matrix that comprises the partial derivatives of the constraint equations at the position level with respect to the vector of coordinates; that is $\partial\boldsymbol{\Phi}/\partial\mathbf{c}$, and $\dot{\mathbf{c}}$ is a 9×1 vector of velocities of the system in the form

$$\dot{\mathbf{c}} = \left\{ \dot{x}_1 \quad \dot{y}_1 \quad \dot{\theta}_1 \quad \dot{x}_2 \quad \dot{y}_2 \quad \dot{\theta}_2 \quad \dot{x}_3 \quad \dot{y}_3 \quad \dot{\theta}_3 \right\}^{\mathrm{T}} \tag{27}$$

The constraint equations at the acceleration level can be obtained by differentiating Eq. (26) with respect to time, yielding

$$\ddot{\mathbf{\Phi}} \equiv \mathbf{D}\ddot{\mathbf{c}} = \boldsymbol{\gamma} \tag{28}$$

where $\boldsymbol{\gamma}$ is an 8×1 vector commonly named right-hand side vector of acceleration constraints that includes the quadratic terms in velocities in the equations of motion, namely the centrifugal parcel. The name, quadratic velocity vector, is due to the existence of the quadratic terms of velocities [53]. A detailed analysis of the constraint equations at the position, velocity and acceleration levels of the slider-crank mechanism can be found in Appendix A.

It is worth noting that the Jacobian matrix $\mathbf{D}$ for the slider-crank mechanism under analysis is an 8×9 coefficient matrix that, by definition, can be obtained by taking the partial derivatives of the constraint equations at the position level (17)-(24) with respect to the vector of coordinates (1), yielding

$$\mathbf{D} = \begin{bmatrix} 1 & 0 & \frac{l_1}{2}\sin\theta_1 & 0 & 0 & 0 & 0 & 0 & 0 \\ 0 & 1 & -\frac{l_1}{2}\cos\theta_1 & 0 & 0 & 0 & 0 & 0 & 0 \\ 1 & 0 & -\frac{l_1}{2}\sin\theta_1 & -1 & 0 & -\frac{l_2}{2}\sin\theta_2 & 0 & 0 & 0 \\ 0 & 1 & \frac{l_1}{2}\cos\theta_1 & 0 & -1 & \frac{l_2}{2}\cos\theta_2 & 0 & 0 & 0 \\ 0 & 0 & 0 & 1 & 0 & -\frac{l_2}{2}\sin\theta_2 & -1 & 0 & 0 \\ 0 & 0 & 0 & 0 & 1 & \frac{l_2}{2}\cos\theta_2 & 0 & -1 & 0 \\ 0 & 0 & 0 & 0 & 0 & 0 & 0 & 1 & 0 \\ 0 & 0 & 0 & 0 & 0 & 0 & 0 & 0 & 1 \end{bmatrix} \tag{29}$$

Comparing Eqs. (16) and (29), it can be observed that the coefficient matrix of the joint reaction forces and moments corresponds to the transpose Jacobian matrix associated with the kinematic joints, that is, the joint reactions vector can have the following form

$$\mathbf{h}_{\mathrm{r}} = -\mathbf{D}^{\mathrm{T}}\boldsymbol{\lambda} \tag{30}$$

A complete description of the relation given by Eq. (30) can be found in Appendix B, for which the d'Alembert's principle is considered [57].

Thus, it is now possible to obtain a linear system of 17 equations with 17 unknowns for the slider-crank system, by appending the equations of motion (12) to the acceleration constraint equations (28). Taking advantage of the relation between coefficient matrix and Jacobian matrix (30), finally the equations of motion of the slider-crank mechanism can be written as

$$\mathbf{M}\ddot{\mathbf{c}} + \mathbf{D}^{\mathrm{T}}\boldsymbol{\lambda} = \mathbf{h}_{\mathrm{a}} \tag{31}$$

$$\mathbf{D}\ddot{\mathbf{c}} = \boldsymbol{\gamma} \tag{32}$$

or, alternatively, in a matrix structure

$$\begin{bmatrix} \mathbf{M} & \mathbf{D}^{\mathrm{T}} \\ \mathbf{D} & \mathbf{0} \end{bmatrix} \begin{Bmatrix} \ddot{\mathbf{c}} \\ \boldsymbol{\lambda} \end{Bmatrix} = \begin{Bmatrix} \mathbf{h}_{\mathrm{a}} \\ \boldsymbol{\gamma} \end{Bmatrix} \tag{33}$$

Equation (33) is formed as a combination of the differential equations of motion (12) and the kinematic algebraic equations at the acceleration level (28), which is often referred to as "mixed set of differential algebraic equations" (DAE) [58]. In fact, Eq. (33) constitutes a system of DAE of index-1 [59] that is linear in the accelerations and in the Lagrange multipliers. The solution of the linear equations presented previously is an initial value problem, requiring the state of the system at some instant of time to be specified [60]. Thus, since all the linear and rotational

components of positions and velocities can be easily established from the characterization of the slider-crank multibody model, the 17 equations (33) can be solved for nine linear and rotational accelerations, $\ddot{\mathbf{c}}$, and eight joint reaction forces and moments, $\boldsymbol{\lambda}$, by using any numerical algorithm for solving systems of linear equations [61]. Then, in each integration time step, the accelerations, $\ddot{\mathbf{c}}$, together with the vector of velocities, $\dot{\mathbf{c}}$, are integrated in time to obtain the system velocities and positions at the next time step. This procedure is repeated up to the final time of dynamic analysis is reached.

It must be noticed that the resolution of the system of equations (33) does not necessarily satisfy the position and velocity constraint equations (25) and (26), because these two sets of equations are not explicitly used in the dynamic analysis procedure. Consequently, for moderate or long simulation time, the initial constraint equations are rapidly violated due to the integration process, namely integration truncation errors. With the purpose of eliminating, or at least minimizing, the constraints violation during the numerical resolution of the equations of motion, any of the available methods in the literature should be utilized. The interested reader is referred to the works by Baumgarte [62], Wehage and Haug [63], Chang and Nikravesh [64], Bayo et al. [65], Kim et al. [66], Yoon et al. [67], Chiou and Wu [68], Yu and Chen [69], Weijia et al. [70], Blajer [71], Neto and Ambrósio [72], Braun and Goldfarb [73], Flores et al. [74], Zhang et al. [75], Marques et al. [76] and Pappalardo et al. [77] for further details on the methods to handle the constraints violation.

Finally, it should be mentioned that the Newton-Euler formulation can be expanded to incorporate other features associated with multibody dynamics, such as complex constraints, spring and damper actuators, drivers, contact and friction phenomena, as well as general procedures to generate, assembly and solve the equations of motion, just to mention a few.

3. Lagrangian formulation

The Lagrangian formulation allows the equations of motion of multibody mechanical systems to be obtained in a simple and straightforward manner, since it is based on scalar quantities, namely kinetic and potential energies, rather than vector variables as in the Newton-Euler methodology. However, this approach has some difficulties when applied to constrained multibody systems with closed loop chains, such as in mechanisms and manipulators. For that reason, in this section, the Lagrangian formulation is revisited and developed from the Newton-Euler approach. In the sequel of this process, the planar slider-crank mechanism, shown in Fig. 1, is considered as a demonstrative application example.

It is well-known that Lagrange established the concept of generalized coordinates, which can be either distances or angles [3, 78]. Similarly, generalized forces can be associated with forces or moments. Broadly, the generalized coordinates are directly related to the degrees-of-freedom that exist in the system under analysis, resulting in a minimum number of equations of motion, reason why this approach is often named as minimal coordinates formulation [79]. Thus, for the slider-crank mechanism, illustrated in Fig. 1, there is one generalized coordinate only, since the system has a single degree-of-freedom. Therefore, the Lagrangian formulation should generate one equation of motion for the slider-crank mechanism. It is clear that for this linkage system, the crank angle would be the obvious choice to be the independent generalized coordinate, which can be represented by

$$q = \{\theta_1\} \tag{34}$$

It must be mentioned that the set of coordinates utilized to develop the equations of motion based on the Lagrangian formulation is not unique, since the coordinates can be related to each other. Thus, for instance, the Cartesian coordinates of the center of mass of the crank may be expressed as functions of the independent generalized coordinates using the following constraint equations

$$x_1 = \frac{l_1}{2}\cos\theta_1 \tag{35}$$

$$y_1 = \frac{l_1}{2}\sin\theta_1 \tag{36}$$

The corresponding velocity constraints can be obtained as the time derivatives of Eqs. (35) and (36), yielding

$$\dot{x}_1 = -\frac{l_1}{2}\sin\theta_1\dot{\theta}_1 \tag{37}$$

$$\dot{y}_1 = \frac{l_1}{2}\cos\theta_1\dot{\theta}_1 \tag{38}$$

or in a compact and generic form as

$$\dot{\mathbf{c}} = \mathbf{W}\dot{\mathbf{q}} \tag{39}$$

where $\dot{\mathbf{c}}$ represents center of mass velocities of the bodies, $\mathbf{W}$ is the transformation matrix, which allows for the relation between the Cartesian and generalized coordinates, and $\dot{\mathbf{q}}$ denotes the generalized velocities. It should be mentioned that, the transformation of coordinates is the central core of the Lagrangian formulation, and small variations or changes in the center of mass coordinates consistent with all the position constraints can be obtained from the virtual displacements in the generalized coordinates, $\delta\mathbf{q}$, as

$$\delta\mathbf{c} = \frac{\partial\mathbf{c}}{\partial\mathbf{q}}\delta\mathbf{q} = \mathbf{W}\delta\mathbf{q} \tag{40}$$

in which there is no partial time derivative multiplied by a time increment, because the system's configuration does not change during a virtual displacement. The most general form of the transformation matrix can be written as [79]

$$\mathbf{W} = \frac{\partial\mathbf{c}}{\partial\mathbf{q}} = \frac{\partial\dot{\mathbf{c}}}{\partial\dot{\mathbf{q}}} \tag{41}$$

It is clear that the mechanical power P of the slider-crank mechanism under analysis may be expressed in terms of either $\dot{\mathbf{c}}$ or $\dot{\mathbf{q}}$, that is

$$P = \mathbf{h}_a^{\mathrm{T}}\dot{\mathbf{c}} \tag{42}$$

$$P = \mathbf{Q}_a^{\mathrm{T}}\dot{\mathbf{q}} \tag{43}$$

where Eq. (43) represents the generalized power associated with generalized applied forces, $\mathbf{Q}_a$, and generalized velocities $\dot{\mathbf{q}}$. Combining Eqs. (39), (42) and (43), it yields the following relation between applied forces, $\mathbf{h}_a$, and generalized forces $\mathbf{Q}_a$,

$$\mathbf{Q}_a = \mathbf{W}^{\mathrm{T}}\mathbf{h}_a \tag{44}$$

Thus, the generalized forces can be easily determined from the knowledge of the center of mass approach using the transformation matrix $\mathbf{W}$.

The key issue of the Lagrangian formulation is the concept of the Lagrangian function related to the system dynamics and, by definition, is expressed as

$$L = T - V \tag{45}$$

where T is the kinetic energy of the system and V is the potential energy of the system.

The kinetic energy of the slider-crank mechanism can be written in terms of the center of mass coordinates as follows

$$T = \frac{1}{2}\dot{\mathbf{c}}^{\mathrm{T}}\mathbf{M}\dot{\mathbf{c}} \tag{46}$$

Differentiating Eq. (46) with respect to the velocities results in

$$\frac{\partial T}{\partial \dot{\mathbf{c}}} = \dot{\mathbf{c}}^{\mathrm{T}}\mathbf{M} \tag{47}$$

Hence, the time derivative of Eq. (47) results in the inertial forces as

$$\frac{\mathrm{d}}{\mathrm{d}t}\left(\frac{\partial T}{\partial \dot{\mathbf{c}}}\right) = \ddot{\mathbf{c}}^{\mathrm{T}}\mathbf{M} \tag{48}$$

where the mass matrix $\mathbf{M}$ is assumed to be constant, since the system does not change the mass.

In turn, the potential forces can, by definition, be expressed as [55]

$$\mathbf{h}_{\mathrm{p}}^{\mathrm{T}} = -\frac{\partial V}{\partial \mathbf{c}} \tag{49}$$

Thus, the generic form of the Lagrange's equations of motion of the slider-crank mechanism, expressed in terms of center of mass coordinates and velocities, can be developed with basis on the kinetic and potential energies as

$$\frac{\mathrm{d}}{\mathrm{d}t}\left(\frac{\partial T}{\partial \dot{\mathbf{c}}}\right) + \frac{\partial V}{\partial \mathbf{c}} = \mathbf{h}_{\mathrm{d}}^{\mathrm{T}} \tag{50}$$

in which the first term represents the inertial forces, the second one denotes the potential forces, such as those associated with gravity and springs, and the right-hand side of Eq. (50) is the term for non-potential, or non-conservative, forces applied to the system. In the most general case, the total applied forces on the system are given by the summation of conservatives and non-conservative forces, i.e., $\mathbf{h}_{\mathrm{a}} = \mathbf{h}_{\mathrm{p}} + \mathbf{h}_{\mathrm{d}}$.

It is appropriate to express the equations of the motion (50) as function of the generalized coordinates, $\mathbf{q}$, and generalized velocities, $\dot{\mathbf{q}}$, that is

$$\frac{\mathrm{d}}{\mathrm{d}t}\left(\frac{\partial T}{\partial \dot{\mathbf{c}}}\right)\frac{\partial \mathbf{c}}{\partial \mathbf{q}} + \frac{\partial V}{\partial \mathbf{c}}\frac{\partial \mathbf{c}}{\partial \mathbf{q}} = \mathbf{Q}_{\mathrm{d}}^{\mathrm{T}} \tag{51}$$

It must be recalled from Calculus of Variations that [80]

$$\frac{\mathrm{d}}{\mathrm{d}t}\left(\frac{\partial T}{\partial \dot{\mathbf{c}}}\frac{\partial \mathbf{c}}{\partial \mathbf{q}}\right) = \frac{\mathrm{d}}{\mathrm{d}t}\left(\frac{\partial T}{\partial \dot{\mathbf{c}}}\right)\frac{\partial \mathbf{c}}{\partial \mathbf{q}} + \frac{\partial T}{\partial \dot{\mathbf{c}}}\frac{\mathrm{d}}{\mathrm{d}t}\left(\frac{\partial \mathbf{c}}{\partial \mathbf{q}}\right) \tag{52}$$

yielding

$$\frac{\mathrm{d}}{\mathrm{d}t}\left(\frac{\partial T}{\partial \dot{\mathbf{c}}}\right)\frac{\partial \mathbf{c}}{\partial \mathbf{q}} = \frac{\mathrm{d}}{\mathrm{d}t}\left(\frac{\partial T}{\partial \dot{\mathbf{c}}}\frac{\partial \mathbf{c}}{\partial \mathbf{q}}\right) - \frac{\partial T}{\partial \dot{\mathbf{c}}}\frac{\mathrm{d}}{\mathrm{d}t}\left(\frac{\partial \mathbf{c}}{\partial \mathbf{q}}\right) \tag{53}$$

Introducing now Eq. (53) into Eq. (51) results in

$$\frac{\mathrm{d}}{\mathrm{d}t}\left(\frac{\partial T}{\partial \dot{\mathbf{c}}}\frac{\partial \mathbf{c}}{\partial \mathbf{q}}\right) - \frac{\partial T}{\partial \dot{\mathbf{c}}}\frac{\mathrm{d}}{\mathrm{d}t}\left(\frac{\partial \mathbf{c}}{\partial \mathbf{q}}\right) + \frac{\partial V}{\partial \mathbf{q}} = \mathbf{Q}_{\mathrm{d}}^{\mathrm{T}} \tag{54}$$

It should be noticed that

$$\frac{\mathrm{d}}{\mathrm{d}t}\left(\frac{\partial \mathbf{c}}{\partial \mathbf{q}}\right) = \frac{\partial}{\partial \mathbf{q}}\left(\frac{\partial \mathbf{c}}{\partial \mathbf{q}}\right)\frac{\mathrm{d}\mathbf{q}}{\mathrm{d}t} = \frac{\partial}{\partial \mathbf{q}}\left(\frac{\partial \mathbf{c}}{\partial \mathbf{q}}\right)\dot{\mathbf{q}} = \frac{\partial \dot{\mathbf{c}}}{\partial \mathbf{q}} \tag{55}$$

Considering now Eq. (41) and (55), the Lagrange's equations of motion (54) can be written in terms of generalized coordinates and generalized velocities as

$$\frac{\mathrm{d}}{\mathrm{d}t}\left(\frac{\partial T}{\partial \dot{\mathbf{q}}}\right)-\frac{\partial T}{\partial \mathbf{q}}+\frac{\partial V}{\partial \mathbf{q}}=\mathbf{Q}_{\mathrm{d}}^{\mathrm{T}} \tag{56}$$

Finally, taking into account the concept of Lagrangian function given by Eq. (45), the Lagrange's equations of motion of second kind in its classical fashion can be expressed as

$$\frac{\mathrm{d}}{\mathrm{d}t}\left(\frac{\partial L}{\partial \dot{\mathbf{q}}}\right)-\frac{\partial L}{\partial \mathbf{q}}=\mathbf{Q}_{\mathrm{d}}^{\mathrm{T}} \tag{57}$$

where L denotes the Lagrangian function of the system, which is the difference between kinetic and potential energies, expressed in terms of the generalized coordinates and their time derivatives, that is, the generalized velocities. The equations represented by (57) are also called as Euler-Lagrange's equations of motion, because although Lagrange was the first to formulate them specifically as the equations of motion, they were previously derived by Euler as the conditions under which a point passes from one specific place and time to another in such a way that the integral of a given Lagrangian function with respect to time is stationary, which represents the principle of minimum action [81].

In order for the slider-crank mechanism to be formulated with Lagrangian approach, it is first necessary to establish the quantities required to obtain the Lagrangian function. This multibody system has one degree-of-freedom, thus, one is also the number of generalized coordinates that uniquely represent the system's configuration, that is, the position and orientation of all bodies. As in the previous section, the bodies have lengths l_i, masses m_i, and moments of inertia I_i, in which i = 1, 2 and 3. Thus, the vector of generalized coordinates and velocities are defined as

$$q=\left\{\theta_1\right\} \tag{58}$$

$$\dot{q}=\left\{\dot{\theta}_1\right\} \tag{59}$$

The first step to derive the Lagrange's equation of motion consists of expressing the center of mass position of bodies in terms of the generalized coordinates. Thus, based on the geometry of the slider-crank mechanism shown in Fig. 1, the position of the center of mass of the crank, connecting rod and slider can be written as

$$x_1=\frac{l_1}{2}\cos\theta_1 \tag{60}$$

$$y_1=\frac{l_1}{2}\sin\theta_1 \tag{61}$$

$$x_2=l_1\cos\theta_1+\frac{l_2}{2}\cos\theta_2 \tag{62}$$

$$y_2=\frac{l_1}{2}\sin\theta_1 \tag{63}$$

$$x_3=l_1\cos\theta_1+l_2\cos\theta_2 \tag{64}$$

$$y_3=0 \tag{65}$$

From the geometric configuration of the slider-crank mechanism, it is clear that the angular coordinate of the connecting rod can be expressed as function of the generalized independent coordinate, θ_1, as

$$\theta_2=\sin^{-1}\left(-\frac{l_1}{l_2}\sin\theta_1\right) \tag{66}$$

The velocities of the center of mass of the crank, connecting rod and slider, expressed in terms of the generalized coordinates and their derivatives, can be obtained by differentiation of Eqs. (60)-(65), yielding

$$\dot{x}_1 = -\frac{l_1}{2}\sin\theta_1\dot{\theta}_1 \tag{67}$$

$$\dot{y}_1 = \frac{l_1}{2}\cos\theta_1\dot{\theta}_1 \tag{68}$$

$$\dot{x}_2 = -l_1\sin\theta_1\dot{\theta}_1 - \frac{l_2}{2}\sin\theta_2\dot{\theta}_2 \tag{69}$$

$$\dot{y}_2 = \frac{l_1}{2}\cos\theta_1\dot{\theta}_1 \tag{70}$$

$$\dot{x}_3 = -l_1\sin\theta_1\dot{\theta}_1 - l_2\sin\theta_2\dot{\theta}_2 \tag{71}$$

$$\dot{y}_3 = 0 \tag{72}$$

where the angular velocity of the connecting rod must be expressed in terms of the generalized coordinates and generalized velocities of the slider-crank mechanism. Therefore, taking the time derivate of Eq. (66), results in

$$\dot{\theta}_2 = -\frac{l_1\cos\theta_1\dot{\theta}_1}{\sqrt{l_2^2 - l_1^2\sin^2\theta_1}} \tag{73}$$

The kinetic energy associated with the slider-crank mechanism bodies can be expressed as

$$T_i = \frac{1}{2}I_i\dot{\theta}_i^2 + \frac{1}{2}m_i\left(\dot{x}_i^2 + \dot{y}_i^2\right), \qquad i = 1, 2, 3 \tag{74}$$

The gravitational potential energy related to each body of the system can be defined as

$$V_i = m_i g y_i, \qquad i = 1, 2, 3 \tag{75}$$

Thus, using the above presented equations and after some basic mathematical manipulation the Lagrangian function can be written as

$$\begin{aligned} L = {} & \frac{1}{2}I_1\dot{\theta}_1^2 + \frac{1}{8}m_1 l_1^2\dot{\theta}_1^2 - \frac{1}{2}m_1 g l_1\sin\theta_1 + \\ & \frac{1}{2}I_2 l_1^2 A\dot{\theta}_1^2 + \frac{1}{2}m_2\left(l_1^2 B + \frac{l_1^4}{4}C + l_1^3 D + \frac{l_1^2}{4}E\right)\dot{\theta}_1^2 - \frac{1}{2}m_2 g l_1\sin\theta_1 + \\ & \frac{1}{2}m_3\left(l_1^2 B + l_1^4 C + 2l_1^3 D\right)\dot{\theta}_1^2 \end{aligned} \tag{76}$$

in which

$$A = \frac{\cos^2\theta_1}{l_2^2 - l_1^2\sin^2\theta_1} \tag{77}$$

$$B = \sin^2\theta_1 \tag{78}$$

$$C = \frac{\sin^2\theta_1\cos^2\theta_1}{l_2^2 - l_1^2\sin^2\theta_1} \tag{79}$$

$$D = \frac{\sin^2\theta_1\cos\theta_1}{\sqrt{l_2^2 - l_1^2\sin^2\theta_1}} \tag{80}$$

$$E = \cos^2\theta_1 \tag{81}$$

The derivatives necessary to achieve the Lagrange's equations of motion for the slider-crank mechanism (57) can be expressed as

$$\frac{\partial L}{\partial \dot{\theta}_1} = I_1\dot{\theta}_1 + \frac{1}{4}m_1 l_1^2\dot{\theta}_1 + I_2 l_1^2 A\dot{\theta}_1 + m_2\left(l_1^2 B + \frac{l_1^4}{4}C + l_1^3 D + \frac{l_1^2}{4}E\right)\dot{\theta}_1 + m_3\left(l_1^2 B + l_1^4 C + 2l_1^3 D\right)\dot{\theta}_1 \tag{82}$$

$$\begin{aligned}\frac{\mathrm{d}}{\mathrm{d}t}\left(\frac{\partial L}{\partial \dot{\theta}_1}\right) = {} & I_1\ddot{\theta}_1 + \frac{1}{4}m_1 l_1^2\ddot{\theta}_1 + \\ & I_2 l_1^2 A\ddot{\theta}_1 + m_2\left(l_1^2 B + \frac{l_1^4}{4}C + l_1^3 D + \frac{l_1^2}{4}E\right)\ddot{\theta}_1 + m_3\left(l_1^2 B + l_1^4 C + 2l_1^3 D\right)\ddot{\theta}_1 + \\ & I_2 l_1^2 \dot{A}\dot{\theta}_1 + m_2\left(l_1^2 \dot{B} + \frac{l_1^4}{4}\dot{C} + l_1^3 \dot{D} + \frac{l_1^2}{4}\dot{E}\right)\dot{\theta}_1 + m_3\left(l_1^2 \dot{B} + l_1^4 \dot{C} + 2l_1^3 \dot{D}\right)\dot{\theta}_1\end{aligned} \tag{83}$$

$$\begin{aligned}\frac{\partial L}{\partial \theta_1} = {} & -\frac{1}{2}m_1 g l_1 \cos\theta_1 + \frac{1}{2}I_2 l_1^2 A'\dot{\theta}_1^2 + \frac{1}{2}m_2\left(l_1^2 B' + \frac{l_1^4}{4}C' + l_1^3 D' + \frac{l_1^2}{4}E'\right)\dot{\theta}_1^2 - \\ & \frac{1}{2}m_2 g l_1 \cos\theta_1 + \frac{1}{2}m_3\left(l_1^2 B' + l_1^4 C' + 2l_1^3 D'\right)\dot{\theta}_1^2\end{aligned} \tag{84}$$

Finally, introducing Eqs. (83) and (84) into Eq. (57), and after mathematical treatment, the Lagrange's equations of the slider-crank mechanism can be written in the form

$$m\ddot{\theta}_1 = h \tag{85}$$

where the inertia and generalized force terms are expressed as

$$\begin{aligned}m = {} & I_1 + I_2\frac{l_1^2\cos^2\theta_1}{l_2^2 - l_1^2\sin^2\theta_1} + \frac{1}{4}\left(m_1 + m_2\cos^2\theta_1\right)l_1^2 + \left(m_2 + m_3\right)l_1^2\sin^2\theta_1 + \\ & \left(\frac{1}{4}m_2 + m_3\right)\frac{l_1^4\sin^2\theta_1\cos^2\theta_1}{l_2^2 - l_1^2\sin^2\theta_1} + \left(m_2 + 2m_3\right)\frac{l_1^3\sin^2\theta_1\cos\theta_1}{\sqrt{l_2^2 - l_1^2\sin^2\theta_1}}\end{aligned} \tag{86}$$

$$\begin{aligned}h = {} & \frac{1}{2}I_2\frac{l_1^2\sin 2\theta_1\left(l_2^2 - l_1^2\right)}{\left(l_2^2 - l_1^2\sin^2\theta_1\right)^2}\dot{\theta}_1^2 + \frac{1}{8}m_2 l_1^2\sin 2\theta_1\dot{\theta}_1^2 - \frac{1}{2}\left(m_2 + m_3\right)l_1^2\sin 2\theta_1\dot{\theta}_1^2 - \\ & \frac{1}{8}\left(m_2 + 4m_3\right)l_1^4\left(\frac{\sin 2\theta_1\cos^2\theta_1}{l_2^2 - l_1^2\sin^2\theta_1} - \frac{\sin 2\theta_1\sin^2\theta_1\left(l_2^2 - l_1^2\right)}{\left(l_2^2 - l_1^2\sin^2\theta_1\right)^2}\right)\dot{\theta}_1^2 - \\ & \frac{1}{2}\left(m_2 + 2m_3\right)l_1^3\left(\frac{\sin 2\theta_1\cos\theta_1 - \sin^3\theta_1}{\sqrt{l_2^2 - l_1^2\sin^2\theta_1}} + \frac{\sin^3\theta_1\cos^2\theta_1 l_1^2}{\left(l_2^2 - l_1^2\sin^2\theta_1\right)^{\frac{3}{2}}}\right)\dot{\theta}_1^2 - \frac{1}{2}\left(m_1 + m_2\right)g l_1\cos\theta_1\end{aligned} \tag{87}$$

A complete and detailed analysis of the Lagrangian formulation for the slider-crank system is presented in Appendix C. It must be mentioned that the equations of motion developed with Lagrangian formulation can be obtained in a straightforward manner, in the measure that the kinematic and potential energies can be easily defined. In fact, according to Lagrange's own words, this formulation involves algebraic operations only, and it does not require any figures, such as the case of free-body diagrams in the Newton-Euler approach [3].

From the analysis of Eq. (85), it can be observed that the Lagrangian formulation results in a set of ordinary differential equations (ODE) that allows for the definition of system's dynamics in terms of generalized coordinates. Therefore, Eq. (85) can be solved and the resulting acceleration integrated in time to obtain the velocity at the next instant of time. The velocity is, then, integrated in order to obtain the system's position. This procedure is repeated up to the final time of simulation is reached. It must be noticed that, in the Lagrangian formulation, there is no violation of constraints, which is an intrinsic merit of this approach.

The Lagrangian formulation leads to less number of equations of motion, when compared, for instance, with Newton-Euler approach; however its form exhibits higher degree of nonlinearity in most of the cases. Nonetheless, the Lagrangian formulation leads to a tedious and overwhelming procedure particularly when modeling closed loop systems.

It must be noticed that the quantity m in Eq. (86) represents the non-constant inertia terms in the Lagrangian formulation for the slider-crank mechanism, as it happens in the case of Newton-Euler method, which can lead to some numerical difficulties when solving the equations of motion. It is worth noting that the inertia terms vary with system's configuration, since they depend on the relative positions of the bodies. In fact, the inertia terms associated with Lagrangian formulation express the relation between the kinetic energy of the system and the derivatives with respect to generalized velocities. Thus, the inertia terms have different dimensions, because Lagrangian formulation utilizes generalized coordinates. In turn, the force parcel, h, given by Eq. (87) include quadratic quantities, namely the centrifugal forces, together with the quantities associated with gravity.

4. Lagrangian formulation with cut joints

One of the great merits of the Lagrangian formulation deals with its simplicity and easiness to derive the equations of motion, because scalar quantities are utilized in the process, namely kinetic and potential energies. However, this formulation can be quite cumbersome when the mechanical system under analysis includes closed loops in its kinematic structure, such as in the case of mechanisms and parallel manipulators. Thus, an interesting and versatile alternative approach to model and simulate multibody mechanical systems with closed loop chains consists of cutting open the closed kinematic structure, and introducing constraints to connect the ends of the bodies at the open joint. This approach results in open systems, which are quite simple and straightforward to model under the umbrella of Lagrangian formulation. Moreover, the introduction of the kinematic constraints associated with the cut procedure is a trivial task, as it will be demonstrated. For this purpose, let consider again the planar slider-crank system, in which one of the joints is cut open, as shown in Fig. 3a. This procedure introduces two extra degrees-of-freedom, hence, the slider-crank mechanism is transformed in a combination of a double pendulum with a slider link. In order to have a proper behavior of the planar slider-crank mechanism, two kinematic constraints must be included in the multibody model to ensure the cut open joint remains closed, reason why this approach can be named as "Lagrangian formulation with cut joints" or with "relative coordinates", that contrasts with the classical Lagrangian formulation when there is no explicit kinematic constraints. The Lagrangian formulation with cut joints has been a very convenient and popular method to model complex systems with closed loop topologies under the framework of multibody system dynamics [53, 83, 84].

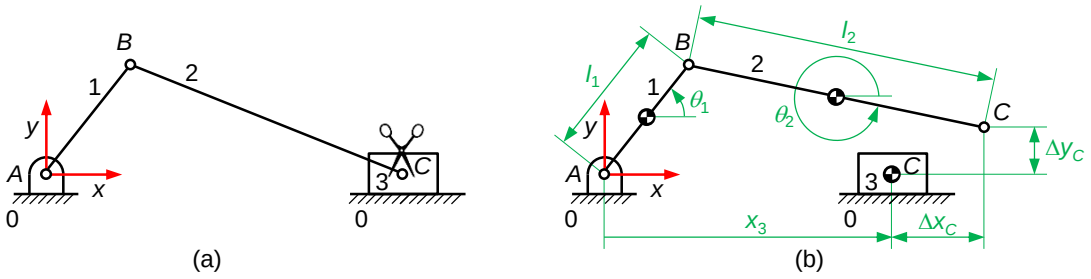

Fig. 3. Slider-crank mechanism and its equivalent model after the cut open procedure.

From the analysis of Fig. 3b, it is clear that the multibody system, which results from the cut open procedure described above, has a total of three degrees-of-freedom, being the independent coordinates defined by the absolute angles of the crank and connecting rod, θ_1 and θ_2, together with the horizontal position of the slider, x_3. Therefore, vectors of generalized coordinates and velocities can be established as

$$\mathbf{q} = \begin{Bmatrix} \theta_1 \\ \theta_2 \\ x_3 \end{Bmatrix} \tag{88}$$

$$\dot{\mathbf{q}} = \begin{Bmatrix} \dot{\theta}_1 \\ \dot{\theta}_2 \\ \dot{x}_3 \end{Bmatrix} \tag{89}$$

With the aim of assemble or close the slider-crank mechanism, and to guarantee its correct dynamic behavior, two kinematic constraints need to be considered to close the loop, namely

$$\Phi_1 \equiv \Delta x_C = 0 \equiv l_1 \cos\theta_1 + l_2 \cos\theta_2 - x_3 = 0 \tag{90}$$

$$\Phi_2 \equiv \Delta y_C = 0 \equiv l_1 \sin\theta_1 + l_2 \sin\theta_2 = 0 \tag{91}$$

or in a compact form as

$$\boldsymbol{\Phi} \equiv \boldsymbol{\Phi}(\mathbf{q}) = \mathbf{0} \tag{92}$$

The second time derivative of Eqs. (90) and (91) yields

$$\ddot{\Phi}_1 \equiv -l_1 \sin\theta_1\ddot{\theta}_1 - l_2 \sin\theta_2\ddot{\theta}_2 - \ddot{x}_3 = l_1 \cos\theta_1\dot{\theta}_1^2 + l_2 \cos\theta_2\dot{\theta}_2^2 \tag{93}$$

$$\ddot{\Phi}_2 \equiv l_1 \cos\theta_1\ddot{\theta}_1 + l_2 \cos\theta_2\ddot{\theta}_2 = l_1 \sin\theta_1\dot{\theta}_1^2 + l_2 \sin\theta_2\dot{\theta}_2^2 \tag{94}$$

which can be written in a compact and matrix form as

$$\ddot{\boldsymbol{\Phi}} \equiv \mathbf{D}\ddot{\mathbf{q}} = \boldsymbol{\gamma} \tag{95}$$

where the Jacobian matrix, vector of generalized accelerations and right-hand side vector of acceleration constraints are given by

$$\mathbf{D} = \begin{bmatrix} -l_1 \sin\theta_1 & -l_2 \sin\theta_2 & -1 \\ l_1 \cos\theta_1 & l_2 \cos\theta_2 & 0 \end{bmatrix} \tag{96}$$

$$\ddot{\mathbf{q}} = \begin{Bmatrix} \ddot{\theta}_1 \\ \ddot{\theta}_2 \\ \ddot{x}_3 \end{Bmatrix} \tag{97}$$

$$\boldsymbol{\gamma} = \begin{Bmatrix} l_1 \cos\theta_1\dot{\theta}_1^2 + l_2 \cos\theta_2\dot{\theta}_2^2 \\ l_1 \sin\theta_1\dot{\theta}_1^2 + l_2 \sin\theta_2\dot{\theta}_2^2 \end{Bmatrix} \tag{98}$$

In order for the slider-crank model to be simulated in the multibody system environment based on the Lagrangian formulation, it is required that the system's equations of motion be derived. For that, let consider the Lagrange's equations of motion of first kind written as [57]

$$\frac{\mathrm{d}}{\mathrm{d}t}\left(\frac{\partial L}{\partial \dot{\mathbf{q}}}\right) - \frac{\partial L}{\partial \mathbf{q}} = \mathbf{Q}_{\mathrm{d}}^{\mathrm{T}} + \mathbf{Q}_{\mathrm{r}}^{\mathrm{T}} \tag{99}$$

where the generalized reaction forces associated with the two kinematic constraints have been incorporated, which can be defined as [79]

$$\mathbf{Q}_{\mathrm{r}} = -\mathbf{D}^{\mathrm{T}}\boldsymbol{\lambda} \tag{100}$$

Once again, the first step to derive the Lagrange's equations of motion for the slider-crank mechanism consists of expressing the bodies' center of mass position in terms of the generalized coordinates (88). Thus, with regard to the information of the slider-crank multibody model presented in Fig. 3, the position of the center of mass of the crank, connecting and slider can be written as

$$x_1 = \frac{l_1}{2}\cos\theta_1 \tag{101}$$

$$y_1 = \frac{l_1}{2}\sin\theta_1 \tag{102}$$

$$x_2 = l_1\cos\theta_1 + \frac{l_2}{2}\cos\theta_2 \tag{103}$$

$$y_2 = l_1\sin\theta_1 + \frac{l_2}{2}\sin\theta_2 \tag{104}$$

$$x_3 = x_3 \tag{105}$$

$$y_3 = 0 \tag{106}$$

In turn, the velocities of the center of mass of the crank, connecting rod and slider, expressed in terms of the generalized coordinates and generalized velocities, can be obtained by simple differentiation of Eqs. (101)-(106), yielding

$$\dot{x}_1 = -\frac{l_1}{2}\sin\theta_1\dot{\theta}_1 \tag{107}$$

$$\dot{y}_1 = \frac{l_1}{2}\cos\theta_1\dot{\theta}_1 \tag{108}$$

$$\dot{x}_2 = -l_1\sin\theta_1\dot{\theta}_1 - \frac{l_2}{2}\sin\theta_2\dot{\theta}_2 \tag{109}$$

$$\dot{y}_2 = l_1\cos\theta_1\dot{\theta}_1 + \frac{l_2}{2}\cos\theta_2\dot{\theta}_2 \tag{110}$$

$$\dot{x}_3 = \dot{x}_3 \tag{111}$$

$$\dot{y}_3 = 0 \tag{112}$$

The kinetic and potential energies associated with the slider-crank mechanism represented in Fig. 3b can be established as

$$T_i = \frac{1}{2}I_i\dot{\theta}_i^2 + \frac{1}{2}m_i\left(\dot{x}_i^2 + \dot{y}_i^2\right), \qquad i = 1, 2, 3 \tag{113}$$

$$V_i = m_i g y_i, \qquad i = 1, 2, 3 \tag{114}$$

Thus, using the above equations relative to the positions and velocities of the bodies' center of mass, and after some basic mathematical manipulation, the Lagrangian function of the slider-crank mechanism can be written as

$$L=\frac{1}{2}\left(I_1+\frac{1}{4}m_1l_1^2+m_2l_1^2\right)\dot{\theta}_1^2+\frac{1}{2}\left(I_2+\frac{1}{4}m_2l_2^2\right)\dot{\theta}_2^2+\frac{1}{2}m_3\dot{x}_3^2+\frac{1}{2}m_2l_1l_2\cos\left(\theta_2-\theta_1\right)\dot{\theta}_1\dot{\theta}_2-\left(\frac{1}{2}m_1+m_2\right)gl_1\sin\theta_1-\frac{1}{2}m_2gl_2\sin\theta_2 \tag{115}$$

The derivatives necessary to obtain the Lagrange's equations of motion for the slider-crank mechanism (99) can be expressed as

$$\frac{\partial L}{\partial\dot{\theta}_1}=\left(I_1+\frac{1}{4}m_1l_1^2+m_2l_1^2\right)\dot{\theta}_1+\frac{1}{2}m_2l_1l_2\cos\left(\theta_2-\theta_1\right)\dot{\theta}_2 \tag{116}$$

$$\frac{\partial L}{\partial\dot{\theta}_2}=\left(I_2+\frac{1}{4}m_2l_2^2\right)\dot{\theta}_2+\frac{1}{2}m_2l_1l_2\cos\left(\theta_2-\theta_1\right)\dot{\theta}_1 \tag{117}$$

$$\frac{\partial L}{\partial\dot{x}_3}=m_3\dot{x}_3 \tag{118}$$

$$\frac{\mathrm{d}}{\mathrm{d}t}\left(\frac{\partial L}{\partial\dot{\theta}_1}\right)=\left(I_1+\frac{1}{4}m_1l_1^2+m_2l_1^2\right)\ddot{\theta}_1+\frac{1}{2}m_2l_1l_2\cos\left(\theta_2-\theta_1\right)\ddot{\theta}_2-\frac{1}{2}m_2l_1l_2\sin\left(\theta_2-\theta_1\right)\dot{\theta}_2\left(\dot{\theta}_2-\dot{\theta}_1\right) \tag{119}$$

$$\frac{\mathrm{d}}{\mathrm{d}t}\left(\frac{\partial L}{\partial\dot{\theta}_2}\right)=\left(I_2+\frac{1}{4}m_2l_2^2\right)\ddot{\theta}_2+\frac{1}{2}m_2l_1l_2\cos\left(\theta_2-\theta_1\right)\ddot{\theta}_1-\frac{1}{2}m_2l_1l_2\sin\left(\theta_2-\theta_1\right)\dot{\theta}_1\left(\dot{\theta}_2-\dot{\theta}_1\right) \tag{120}$$

$$\frac{\mathrm{d}}{\mathrm{d}t}\left(\frac{\partial L}{\partial\dot{x}_3}\right)=m_3\ddot{x}_3 \tag{121}$$

$$\frac{\partial L}{\partial\theta_1}=\frac{1}{2}m_2l_1l_2\sin\left(\theta_2-\theta_1\right)\dot{\theta}_1\dot{\theta}_2-\left(\frac{1}{2}m_1+m_2\right)gl_1\cos\theta_1 \tag{122}$$

$$\frac{\partial L}{\partial\theta_2}=-\frac{1}{2}m_2l_1l_2\sin\left(\theta_2-\theta_1\right)\dot{\theta}_1\dot{\theta}_2-\frac{1}{2}m_2gl_2\cos\theta_2 \tag{123}$$

$$\frac{\partial L}{\partial x_3}=0 \tag{124}$$

Incorporating Eqs. (119)-(124) into Eq. (99), after mathematical treatment, the Lagrange's equations of motion for the slider-crank model of Fig. 3b read

$$\begin{bmatrix}m_{11}&m_{12}&m_{13}\\m_{21}&m_{22}&m_{23}\\m_{31}&m_{32}&m_{33}\end{bmatrix}\begin{Bmatrix}\ddot{\theta}_1\\\ddot{\theta}_2\\\ddot{x}_3\end{Bmatrix}=\begin{Bmatrix}h_1\\h_2\\h_3\end{Bmatrix}-\mathbf{D}^{\mathrm{T}}\boldsymbol{\lambda} \tag{125}$$

in which

$$m_{11}=I_1+\frac{1}{4}m_1l_1^2+m_2l_1^2 \tag{126}$$

$$m_{12} = m_{21} = \frac{1}{2} m_2 l_1 l_2 \cos\left(\theta_2 - \theta_1\right) \tag{127}$$

$$m_{13} = m_{31} = m_{23} = m_{32} = 0 \tag{128}$$

$$m_{22} = I_2 + \frac{1}{4} m_2 l_2^2 \tag{129}$$

$$m_{33} = m_3 \tag{130}$$

$$h_1 = \frac{1}{2} m_2 l_1 l_2 \sin\left(\theta_2 - \theta_1\right) \dot{\theta}_2^2 - \left(\frac{1}{2} m_1 + m_2\right) g l_1 \cos\theta_1 \tag{131}$$

$$h_2 = -\frac{1}{2} m_2 l_1 l_2 \sin\left(\theta_2 - \theta_1\right) \dot{\theta}_1^2 - \frac{1}{2} m_2 g l_2 \cos\theta_2 \tag{132}$$

$$h_3 = 0 \tag{133}$$

At this stage, it must be recalled that the inertia matrix (125) is positive-definite and varies with system's configuration, since in the Lagrangian formulation the inertia relates the kinetic energy of the system with the derivatives with respect to generalized velocities. The generalized force terms (131)-(133) incorporates the quadratic quantities and terms related to gravity.

In dynamic analysis of the slider-crank mechanism represented in Fig. 3b, a unique solution is obtained when the algebraic constraint equations at the acceleration level (95) are considered simultaneously with differential equations of motion (99), together with a set of appropriate initial conditions for generalized coordinates and velocities. Therefore, the resulting Lagrange's equations of motion for the planar slider-crank mechanism with cut joints can be expressed in the matrix structure as

$$\begin{bmatrix} \mathbf{M} & \mathbf{D}^{\mathrm{T}} \\ \mathbf{D} & \mathbf{0} \end{bmatrix} \begin{Bmatrix} \ddot{\mathbf{q}} \\ \boldsymbol{\lambda} \end{Bmatrix} = \begin{Bmatrix} \mathbf{Q}_{\mathrm{d}}^{\mathrm{T}} \\ \boldsymbol{\gamma} \end{Bmatrix} \tag{134}$$

Equation (134) forms a set of five differential algebraic equations (DAE) that can be solved for the three generalized accelerations, $\ddot{\mathbf{q}}$, and the two Lagrange multipliers, $\boldsymbol{\lambda}$, associated with the two cut joint constraints (90) and (91). Then, the generalized velocities and coordinates at the next time step can be obtained by using any available numerical integration scheme [80]. This procedure is repeated up to the final time of simulation is reached. Since Eq. (134) does not explicitly use the constraint equations at the position and velocity levels, thus during the numerical resolution of those equations of motion, the original constraint equations start to be violated due to the integration process or inappropriate initial conditions. Therefore, any of the methods able to eliminate or minimize the errors in the position and velocity constraint equations must be adopted in this context [76].

5. Lagrangian formulation with clearance joint constraint

An alternative approach that can be considered for the modeling process of closed loop multibody systems deals with the incorporation of a clearance joint, which converts them into open systems. Once again, the key point of this procedure is to avoid the complicated and tedious analysis of system with closed topologies when applying the Lagrangian formulation. With the objective to describe the Lagrangian formulation with clearance joints, let, once again, consider the planar slider-crank mechanism as a demonstrative application example. Figure 4a shows a slider-crank mechanism with a revolute clearance joint between the connecting rod and slider, where the clearance size is exaggerated for illustrative purpose.

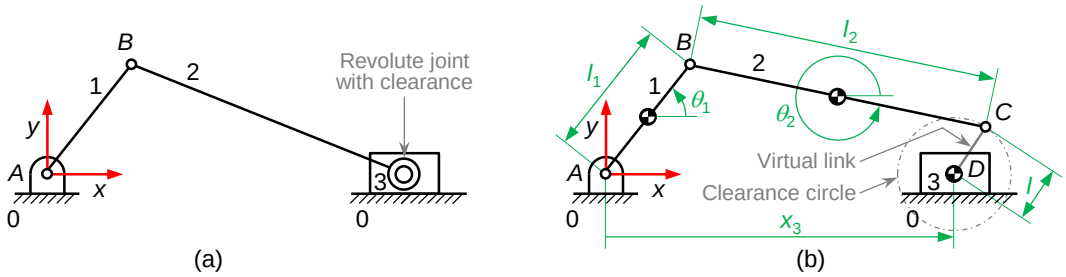

Fig. 4. Slider-crank mechanism with a revolute clearance joint modeled as a virtual or massless link.

One simple way to model a clearance joint consists of considering the massless link approach [82], in which the existence of the clearance at the joint is incorporated by adding a virtual or imaginary rigid body without mass and with a fixed length equal to the clearance size, as it is illustrated in the representation of Fig. 4b. The inclusion of this additional virtual body introduces an extra degree-of-freedom, which can be easily modeled using a constant length constraint [53].

Since the slider-crank mechanism with a revolute clearance joint is as an open system, then the absolute angle of the crank and connecting rod, together with the horizontal position of the slider can be utilized as independent coordinates. Therefore, the vectors of generalized coordinates and generalized velocities can be defined by Eqs. (88) and (89), respectively. Thus, the application of the Lagrange's equations to this multibody system leads to Eq. (125). With the aim of incorporating the virtual link in the spirit of Lagrangian formulation, let consider a constant length constraint to model the revolute clearance joint. For this purpose, and based on the information represented in Fig.4b, one constraint equation can be written as

$$\Phi_1 \equiv \left(x_D - x_C\right)^2 + \left(y_D - y_C\right)^2 - l^2 = 0 \tag{135}$$

where l is the constant distance between points C and D, that is, the clearance size. The Cartesian coordinates of these two points, C and D, can be expressed in terms of the generalized coordinates as

$$x_C = l_1 \cos\theta_1 + l_2 \cos\theta_2 \tag{136}$$

$$y_C = l_1 \sin\theta_1 + l_2 \sin\theta_2 \tag{137}$$

$$x_D = x_3 \tag{138}$$

$$y_D = 0 \tag{139}$$

Thus, the constraint Eq. (135) can be expressed as function of the generalized coordinates as

$$\Phi_1 \equiv \left(x_3 - l_1 \cos\theta_1 - l_2 \cos\theta_2\right)^2 + \left(-l_1 \sin\theta_1 - l_2 \sin\theta_2\right)^2 - l^2 = 0 \tag{140}$$

In a similar way to the case of Lagrangian formulation with cut joints, described in the previous section, the second time derivative of Eq. (140) must be evaluated, yielding

$$\ddot{\Phi}_1 \equiv \mathbf{D}\ddot{\mathbf{q}} = \gamma \tag{141}$$

where

$$\mathbf{D} = \begin{bmatrix} 2\left(x_3 l_1 \sin\theta_1 + l_1 l_2 \sin\left(\theta_2 - \theta_1\right)\right) \\ 2\left(x_3 l_2 \sin\theta_2 + l_1 l_2 \sin\left(\theta_1 - \theta_2\right)\right) \\ 2\left(x_3 - l_1 \cos\theta_1 - l_2 \cos\theta_2\right) \end{bmatrix}^{\mathrm{T}} \tag{142}$$

$$\ddot{\mathbf{q}} = \begin{Bmatrix} \ddot{\theta}_1 \\ \ddot{\theta}_2 \\ \ddot{x}_3 \end{Bmatrix} \tag{143}$$

$$\begin{aligned} \gamma = \Big\{ & -2\left(\dot{x}_3 + 2l_1 \sin\theta_1\dot{\theta}_1 + 2l_2 \sin\theta_2\dot{\theta}_2\right)\dot{x}_3 + \\ & 2l_1 l_2 \cos\left(\theta_2 - \theta_1\right)\left(\dot{\theta}_1^2 + \dot{\theta}_2^2 - 2\dot{\theta}_1\dot{\theta}_2\right) - \\ & 2x_3\left(l_1 \cos\theta_1\dot{\theta}_1^2 + l_2 \cos\theta_2\dot{\theta}_2^2\right)\Big\} \end{aligned} \tag{144}$$

Finally, considering Eqs. (99), (100) and (125), the Lagrange's equations of motion of the slider-crank mechanism with a revolute clearance joint are given by

$$\begin{bmatrix} \mathbf{M} & \mathbf{D}^{\mathrm{T}} \\ \mathbf{D} & 0 \end{bmatrix} \begin{Bmatrix} \ddot{\mathbf{q}} \\ \lambda \end{Bmatrix} = \begin{Bmatrix} \mathbf{Q}_{\mathrm{d}}^{\mathrm{T}} \\ \gamma \end{Bmatrix} \tag{145}$$

Equation (145) represents the equations of motion of the slider-crank mechanism in which the number of selected coordinates is higher than the number of degrees-of-freedom of the system. In fact, Eq. (145) forms a set of four DAE that can be solved for the three generalized accelerations, $\ddot{\mathbf{q}}$, and one Lagrange multiplier, λ, as function of time, given the appropriate initial conditions for the generalized coordinates and velocities. The remaining procedures to solve the equations of motion are exactly the same as discussed in the previous section.

6. Lagrangian formulation with elastic joints

The incorporation of an elastic or flexible joint in multibody mechanical systems allows for a certain amount of play due to the local elastic deformation [85]. As a consequence of this aspect, the existence of an elastic joint in multibody systems with closed topologies permits to transform them into open systems, which eventually, simplifies their modeling process when the Lagrangian formulation is utilized. In order to show the main aspects related to this alternative approach to handle multibody mechanical systems with closed loop kinematic structures, let consider the slider-crank mechanism as a demonstrative example of application example. Figure 5a depicts a planar slider-crank mechanism with an elastic, flexible or bushing joint [85, 86].

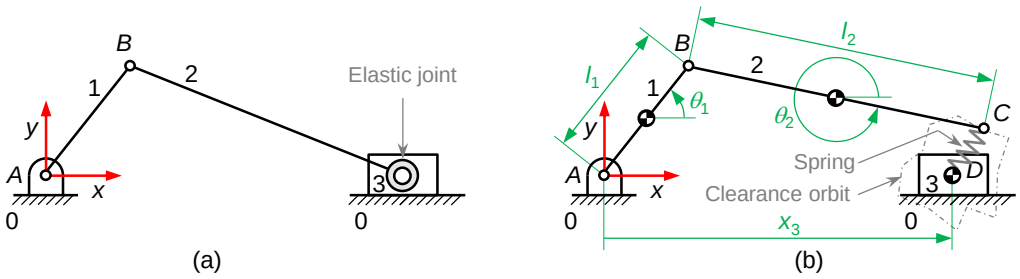

Fig. 5. Slider-crank mechanism with as elastic joint modeled as a spring.

An elastic joint can be incorporated in a multibody model much like as a spring, as it is shown in the representation of Fig. 5b, where a revolute joint is replaced by that spring element. This procedure adds two extra degrees-of-freedom to the system, being the response of the joint controlled by forces rather than kinematic constraints as in the case of ideal or perfect joints. It is clear that a kinematic joint in a multibody system imposes restrictions at the kinematic level to the adjacent bodies, while an elastic or flexible joint leads to force constraints [87-92]. From the operating conditions point of view, it can be observed that for a large value of spring stiffness, the two spring connecting points, *C* and *D*, do not separate from each other in a significant

manner, and, therefore, the closed loop kinematic structure of the slider-crank mechanism is ensured.

In a similar way to the previous section, the slider-crank mechanism with an elastic joint constitutes an open system with three degrees-of-freedom. Therefore, the vector of generalized coordinates and generalized velocities can be established by Eqs. (88) and (89), respectively. The spring element can be easily incorporated in the Lagrange's equations of motion (57) in terms of elastic potential energy, since a spring element represents a conservative force. In fact, the elastic potential energy associated with a spring can be evaluated as

$$V_{\mathrm{s}} = \frac{1}{2} k \left\| \boldsymbol{\Delta} \right\|^2 = \frac{1}{2} k \left(\Delta_x^2 + \Delta_y^2 \right) \tag{146}$$

where k represents the spring stiffness and Δ denotes the elongation of the spring, which, with regard to Fig. 5b, can be expressed in terms of the generalize coordinates as

$$\Delta_x = l_1 \cos\theta_1 + l_2 \cos\theta_2 - x_3 \tag{147}$$

$$\Delta_y = l_1 \sin\theta_1 + l_2 \sin\theta_2 \tag{148}$$

The Lagrangian function for the slider-crank mechanism with an elastic joint represented in Fig. 5b can be defined as

$$L = T_i - V_i - V_{\mathrm{s}}, \qquad i = 1, 2, 3 \tag{149}$$

in which the kinetic energy and the gravitational potential energy have the same expressions as in the previous section, being the elastic potential energy given by Eq. (146).

Thus, the contribution of the elastic joint to the Lagrangian formulation of the slider-crank mechanism depicted in Fig. 5b can be evaluated as

$$\frac{\partial V_{\mathrm{s}}}{\partial \theta_1} = -l_1 \sin\theta_1 k\Delta_x + l_1 \cos\theta_1 k\Delta_y \tag{150}$$

$$\frac{\partial V_{\mathrm{s}}}{\partial \theta_2} = -l_2 \sin\theta_2 k\Delta_x + l_2 \cos\theta_2 k\Delta_y \tag{151}$$

$$\frac{\partial V_{\mathrm{s}}}{\partial x_3} = -k\Delta_x \tag{152}$$

Finally, introducing Eqs. (119)-(124), (150)-(152) into Eq.(57), it yields

$$\begin{bmatrix} m_{11} & m_{12} & m_{13} \\ m_{21} & m_{22} & m_{23} \\ m_{31} & m_{32} & m_{33} \end{bmatrix} \begin{Bmatrix} \ddot{\theta}_1 \\ \ddot{\theta}_2 \\ \ddot{x}_3 \end{Bmatrix} = \begin{Bmatrix} h_1 \\ h_2 \\ h_3 \end{Bmatrix} \tag{153}$$

where the inertia terms of the mass matrix are given by Eqs. (126)-(130). In turn, the generalized force terms for the slider-crank mechanism with an elastic joint are written in the following form

$$h_1 = \frac{1}{2} m_2 l_1 l_2 \sin\left(\theta_2 - \theta_1\right) \dot{\theta}_2^2 - \left(\frac{1}{2} m_1 + m_2 \right) g l_1 \cos\theta_1 + l_1 \sin\theta_1 k\Delta_x - l_1 \cos\theta_1 k\Delta_y \tag{154}$$

$$h_2 = -\frac{1}{2} m_2 l_1 l_2 \sin\left(\theta_2 - \theta_1\right) \dot{\theta}_1^2 - \frac{1}{2} m_2 g l_2 \cos\theta_2 + l_2 \sin\theta_2 k\Delta_x - l_2 \cos\theta_2 k\Delta_y \tag{155}$$

$$h_3 = k\Delta_x \tag{156}$$

in which Δ_x and Δ_y are given by Eqs. (147) and (148).

In contrast with the cut joints and clearance joints approaches, the Lagrangian formulation with elastic joints results in a set of ordinary differential equations of motion for the case of the slider-crank mechanism, because the elastic joint is incorporated into the equations of motion via elastic potential energy that is the basis of the Lagrange's equation (57). With the Lagrangian formulation with elastic joints there is no kinematic constraints, being the resolution of the equations of motion efficient, and, therefore, it is not required any additional method to handle the violation of constraints as the case of the two previous formulations described in sections 4 and 5. However, the definition of the value of the stiffness of the spring element can introduce some numerical instability in the resolution of the equations of motion. In short, the dynamic equations of motion (153) can be solved for the three generalized accelerations, $\ddot{\mathbf{q}}$, and, subsequently, the generalized velocities and generalized positions at the next time step can be obtained in a similar fashion as it was described previously.

An extension of this methodology is the contact mechanics approach that utilizes a dissipative Hertzian-based normal contact and friction models [93-97]. These approaches are similar to the elastic joint approach except that the springs/dampers are of nonlinear nature.

7. Results and discussion

The performance of the five formulations described is compared through the dynamic simulation of the slider-crank mechanism whose geometric and inertia properties and initial conditions are presented in section 2. The Newton-Euler approach with Cartesian coordinates is taken as the reference to be compared with the Lagrangian formulation as well as the Lagrangian formulations in which one joint is cut open to increase the number of degrees-of-freedom and, consequently, coordinates, namely the cut joint, the clearance joint constraint and the elastic joint approaches. The total simulation time is set to 0.13 s, which represents approximately two full rotations of the crank for the initial conditions, and the time integration process is performed using the Euler's method. The remaining parameters utilized in the dynamic simulations are listed in Table 2.

Table 2. Parameters for dynamic simulations.

Parameter	Value
Gravitational acceleration, g	9.81 m/s^2
Integration time step, Δt	10^{-7} s
Radial clearance, l	0.1 mm
Spring stiffness, k	10^6 N/m

The output motion of the mechanism is analyzed through the kinematics of the slider, namely its longitudinal position, velocity and acceleration. Each quantity is presented by four different plots, in which the Newton-Euler approach is compared with each proposed Lagrangian formulation. Figure 6 depicts the position of the slider, and similar macroscopic results are obtained for the five methodologies. The existing differences are not comparable with the global motion of the slider and they are originated by the joint compliance in the elastic approach and the massless link size in the clearance joint model. The remaining formulations present equivalent results with even smaller differences justified by the position constraints violation. In what concerns the longitudinal velocity of the slider, the elastic joint approach shows a clearly different behavior with high frequency oscillation, while the other methods have similar response, as depicted in Fig. 7. The same tendency is demonstrated by the longitudinal acceleration of slider for which the discrepancies of the elastic joint model are more conspicuous, as exhibited in Fig. 8. The Lagrangian formulation with clearance joint also reveals some minor oscillations relatively to the Newton-Euler approach.

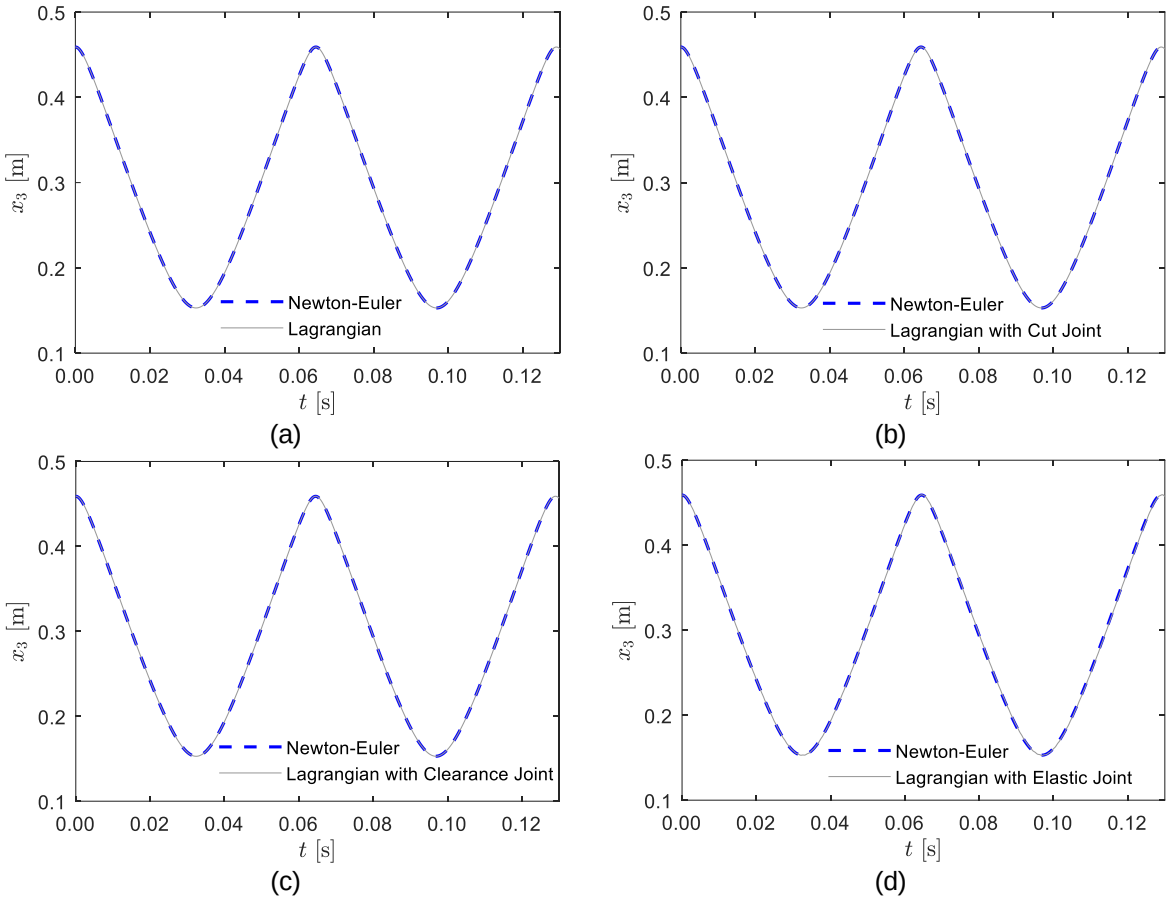

Fig. 6. Longitudinal position of the slider using Newton-Euler method compared with (a) Lagrangian, (b) Lagrangian with cut joint, (c) Lagrangian with clearance joint, (d) Lagrangian with elastic joint.

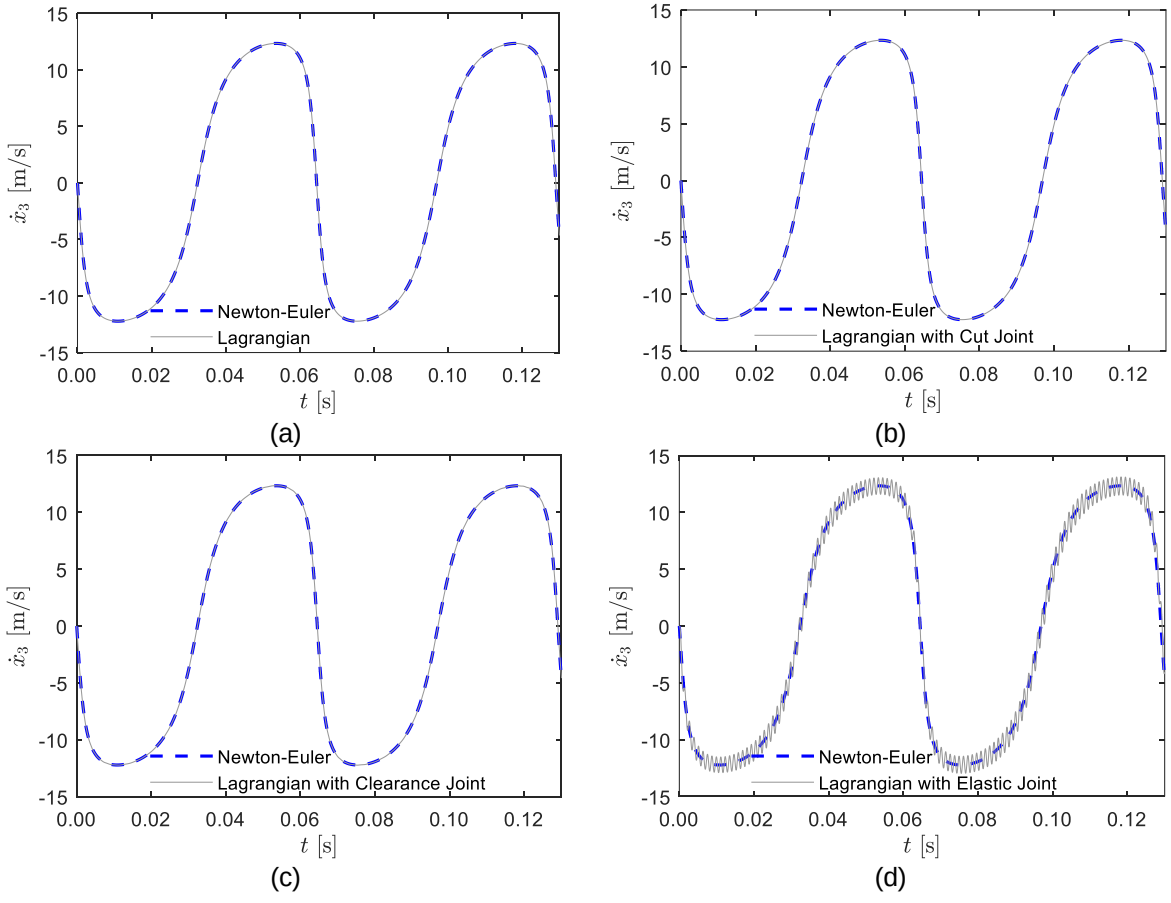

Fig. 7. Longitudinal velocity of the slider using Newton-Euler method compared with (a) Lagrangian, (b) Lagrangian with cut joint, (c) Lagrangian with clearance joint, and (d) Lagrangian with elastic joint.

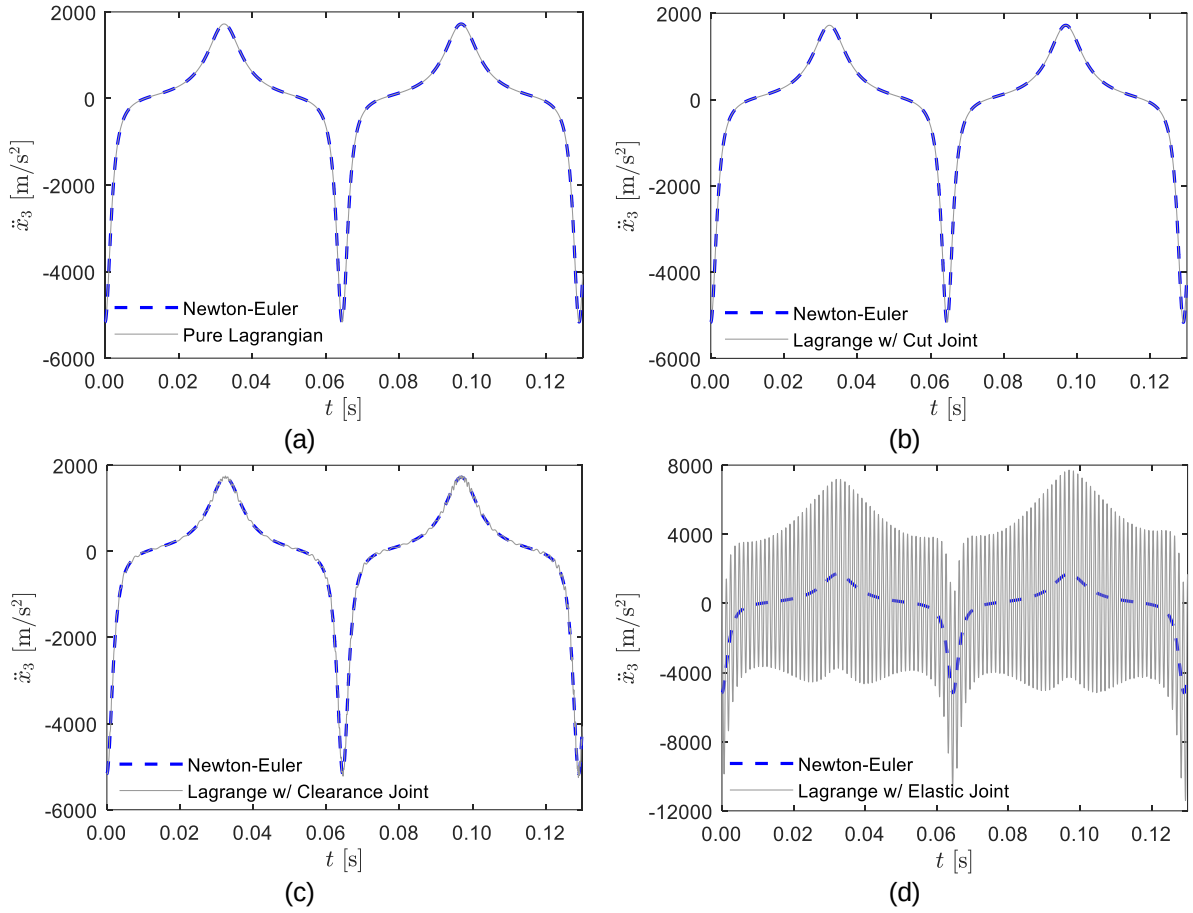

Fig. 8. Longitudinal acceleration of the slider using Newton-Euler method compared with (a) Lagrangian, (b) Lagrangian with cut joint, (c) Lagrangian with clearance joint, and (d) Lagrangian with elastic joint.

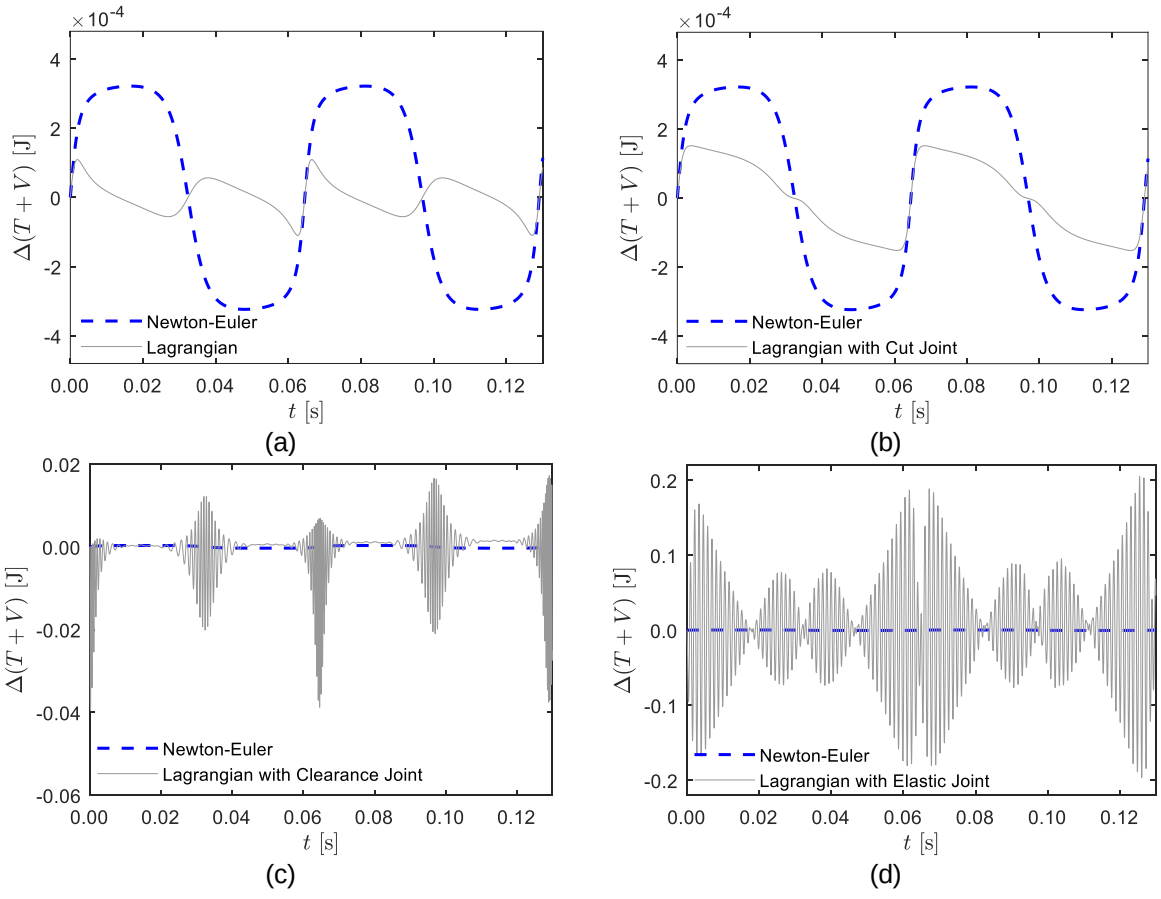

Fig. 9. Mechanical energy variation using Newton-Euler method compared with (a) Lagrangian, (b) Lagrangian with cut joint, (c) Lagrangian with clearance joint, and (d) Lagrangian with elastic joint.

Since no dissipative elements are introduced in any of the presented formulations, it is expected to achieve conservation of the mechanical energy of the system for all cases. In that sense, the variation of mechanical energy relatively to the initial state is displayed in Fig. 9. All methodologies seem to have a cyclic variation of mechanical energy and the lowest level oscillation is obtained with the pure Lagrangian formulation. The Lagrangian formulation with cut joint presents a slightly higher energy variation, which is still lower than with the Newton-Euler approach. The clearance and elastic joint methodologies show significantly higher energy fluctuation which is, respectively, two and three orders of magnitude above the results obtained with the previous methods.

The magnitude of the force between the connecting rod and the slider at joint *C* is presented in Fig. 10 as function of the crank angle. The reaction force in the joint can be directly obtained for the Newton-Euler, the cut joint and the clearance joint approaches during the resolution of the equations of motion through the Lagrange multipliers. It must be noted that, for the clearance joint model, since the units of Eq. (140) are m^2, the calculated Lagrange multiplier does not return exactly a force and, therefore, needs to be normalized. Regarding the Lagrangian formulation, only the angular motion of the crank is obtained in the dynamic simulation, thus, an inverse dynamic analysis is required to compute the force at the joint. In the elastic joint approach, the force is calculated though the spring deformation. Figure 10 exhibits identical results for the Newton-Euler, Lagrangian and Lagrangian with cut joint. For the clearance joint model, small fluctuations of the joint force with high frequency are identified and, for the elastic joint approach, the most prominent differences are found where the maximum force achieves twice the magnitude compared with the previous cases.

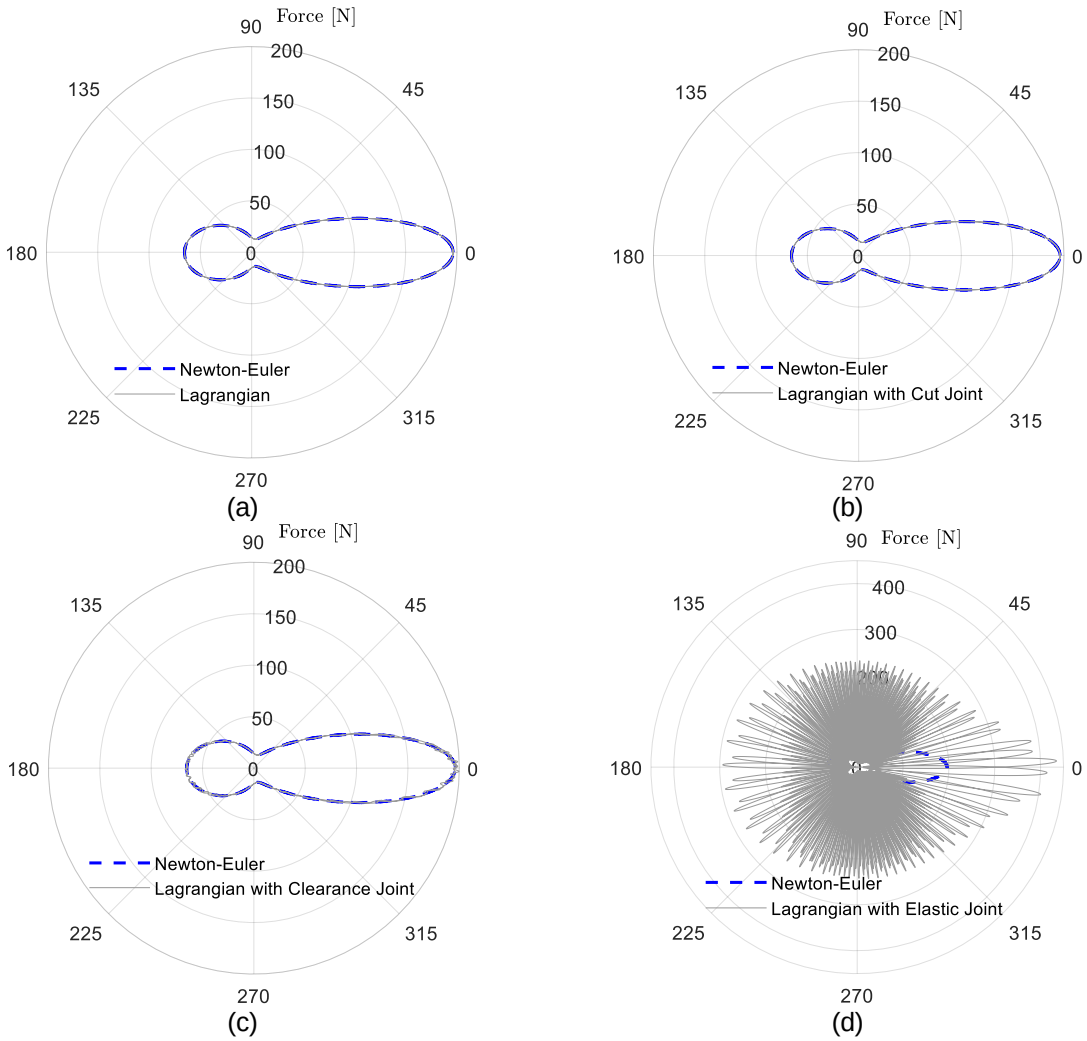

Fig. 10. Contact force magnitude at joint C as function of the crank rotation angle using Newton-Euler method compared with (a) Lagrangian, (b) Lagrangian with cut joint, (c) Lagrangian with clearance joint, and (d) Lagrangian with elastic joint.

The computational efficiency of the different modelling techniques for the slider-crank mechanism is evaluated using the Euler integration algorithm with a time step of $\Delta t = 10^{-7}$ s for all simulations. Thus, the time ratio relatively to the Newton-Euler approach is presented in Fig. 11, as well as the segmentation of the different calculation steps. Moreover, the percentage of time spent in each computation phase is also detailed in Table 3. The results demonstrate that the Newton-Euler approach is clearly the most expensive method from the computational point of view when equal number of evaluations of the equations of motion is considered. On the other hand, the Lagrangian formulation presents a much higher efficiency with approximately ten times less computational time, which results from the minimal number of coordinates and, consequently, equations of motion. The utilization of cut joint or clearance joint present similar simulation time with 67% and 61% of the time spent by Newton-Euler approach, respectively, while the elastic joint model takes around 36%. A closer look at the time spent in each calculation step can justify the discrepancies obtained between all formulations. It is demonstrated that the resolution of the equations of motion corresponds to a large share of computation time, mainly in the Newton-Euler approach, and it is dramatically reduced when using the Lagrangian formulation. The assemble of the system of equations of motion, i.e., joining the dynamic equations with the constraint equations also represents a significant amount of the computational cost, which is saved in the Lagrangian formulation and in the elastic joint approach. It must be noted that, although the generalized forces vector requires significantly more computation time in the Lagrangian formulation due to its nonlinear nature, it is largely compensated by the time saved in the remaining steps.

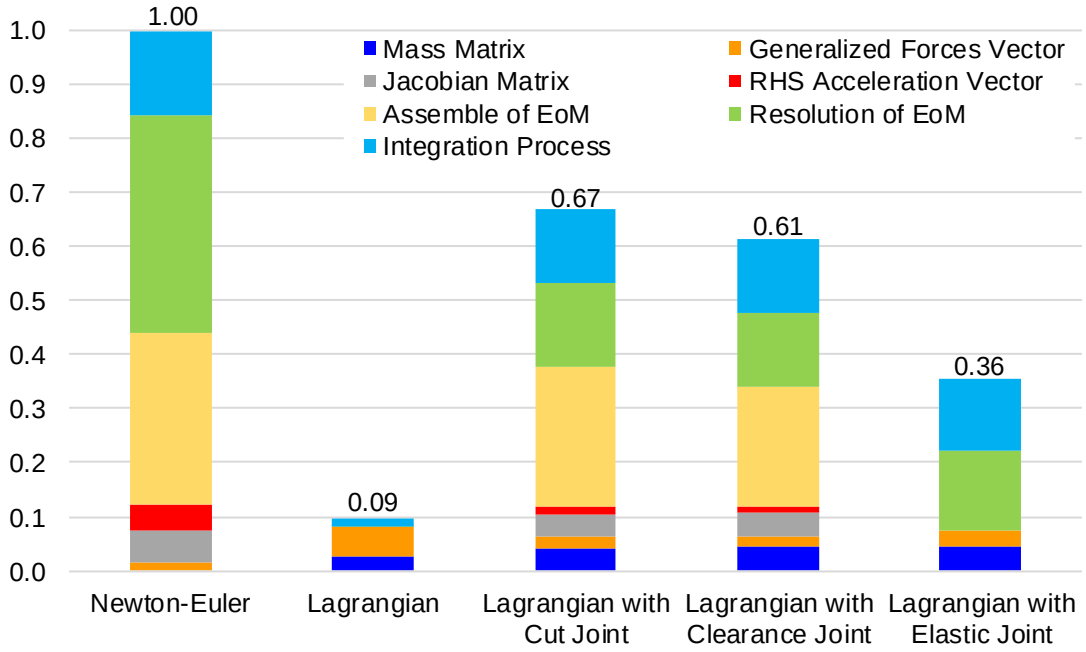

Fig. 11. Simulation time ratio with respect to the Newton-Euler method and segmentation for different calculation steps.

The previously presented results consider a constant time step of integration to produce a reasonable comparison between methodologies. However, each formulation might require a different time step according to its characteristics. Bearing that in mind, an analysis of the influence of the time step in the accuracy of the results was performed, in which two different quantities are evaluated for four different time step values. First, the sum of the position violation of constraints at the final time of simulations is displayed in Table 4, which is not applicable to the Lagrangian formulation nor the Lagrangian formulation with elastic joint. Then, the average absolute variation of the mechanical energy of the system is presented in Table 5.

Table 3. Time consumed in each calculation step for all formulations.

Calculation Step	Newton-Euler	Lagrangian	Lagrangian with Cut Joint	Lagrangian with Clearance Joint	Lagrangian with Elastic Joint
Mass Matrix	NA	27%	6%	7%	13%
Generalized Forces Vector	1%	58%	3%	3%	8%
Jacobian Matrix	6%	NA	6%	7%	NA
RHS Vector of Accelerations*	5%	NA	2%	1%	NA
Assemble of Equations of Motion	32%	NA	38%	36%	NA
Resolution of Equations of Motion	40%	1%	23%	23%	42%
Integration Process	16%	14%	20%	22%	38%

* right-hand side vector of accelerations

Table 4. Sum of the position violation of constraints [m] at the end of the simulations for different integration steps

Δt [s]	Newton-Euler	Lagrangian	Lagrangian with Cut Joint	Lagrangian with Clearance Joint	Lagrangian with Elastic Joint
10^{-5}	$2.85 \cdot 10^{-3}$	NA	$2.85 \cdot 10^{-3}$	*	NA
10^{-6}	$2.85 \cdot 10^{-4}$		$2.85 \cdot 10^{-4}$	*	
10^{-7}	$2.85 \cdot 10^{-5}$		$2.85 \cdot 10^{-5}$	$8.03 \cdot 10^{-5}$	
10^{-8}	$2.85 \cdot 10^{-6}$		$2.85 \cdot 10^{-6}$	$2.49 \cdot 10^{-5}$	

* The simulation did not reach the end since the mechanism presented a close to singular Jacobian matrix

Table 5. Average absolute variation of mechanical energy [J] during the simulation for different integration steps

Δt [s]	Newton-Euler	Lagrangian	Lagrangian with Cut Joint	Lagrangian with Clearance Joint	Lagrangian with Elastic Joint
10^{-5}	$2.62 \cdot 10^{-2}$	$3.94 \cdot 10^{-3}$	$9.87 \cdot 10^{-3}$	*	$1.69 \cdot 10^{5}$
10^{-6}	$2.62 \cdot 10^{-3}$	$3.94 \cdot 10^{-4}$	$9.86 \cdot 10^{-4}$	*	$2.23 \cdot 10^{-1}$
10^{-7}	$2.62 \cdot 10^{-4}$	$3.94 \cdot 10^{-5}$	$9.85 \cdot 10^{-5}$	$2.95 \cdot 10^{-2}$	$5.06 \cdot 10^{-2}$
10^{-8}	$2.62 \cdot 10^{-5}$	$3.94 \cdot 10^{-6}$	$9.85 \cdot 10^{-6}$	$2.57 \cdot 10^{-3}$	$4.64 \cdot 10^{-2}$

* The simulation did not reach the end since the mechanism presented a close to singular Jacobian matrix

Regarding the violation of constraints, both the Newton-Euler and the Lagrangian with cut joint exhibit the same level of violation, which decreases proportionally to the time step. The Lagrangian formulation with clearance joint shows a higher level of violation due to the nature of the kinematic constraint. It must be highlighted that, with this methodology, the use of a larger time step leads to a configuration in which the Jacobian matrix can become singular and, therefore, the equations of motion cannot be solved. This issue is closely linked with the size of the massless link, i.e., if the clearance size is increased, this problem tends to be avoided.

In what concerns the mechanical energy variation, all formulations except the Lagrangian with elastic joint exhibit a reduction with the same order of magnitude of the decrease of the time step. As previously demonstrated in the results of Fig. 9, for the same time step, the Lagrangian formulation shows the lowest variation of mechanical energy followed by the Lagrangian with cut joint, Newton-Euler and, then, Lagrangian with clearance joint. The results presented in Table 5 show that the same relative performance can be achieved with a different step size. Regarding the Lagrangian formulation with elastic joint, the need of a given time step is closely linked with the defined spring stiffness; i.e., a stiffer joint requires a smaller time step, otherwise it can lead to high energy gains as shown in the Table 5.

These results could be expanded to other studies in which the modeling of slider-crank mechanisms is required [98-103].

Table 6. Comparison between the characteristics of the five formulations utilized to model the slider-crank mechanism.

Category	Topic	Formulation				
		Newton-Euler	Lagrangian			
			Classical	with Cut Joint	with Clearance Joint	with Elastic Joint
Formulation	Conceptual Basis	Force Equilibrium	Energy Balance	Energy Balance	Energy Balance	Energy Balance
	Dependent on the Reference Coordinate Frame	Yes	No	Yes	Yes	Yes
	Determination of All State Variables of the System	Intrinsic	Req. Addit. Calc.*	Req. Addit. Calc.*	Req. Addit. Calc.*	Req. Addit. Calc.*
Coordinates	Generalized Coordinates	Dependent	Independent	Dependent	Dependent	Dependent
	Number of Generalized Coordinates	Large	Minimum	Moderate	Moderate	Moderate
	Number of Constraint Equations	Large	None	Reduced	Reduced	Reduced
Equations of Motion	Type of Equations of Motion	DAE	ODE	DAE	DAE	ODE
	Constraint Equations	Yes	No	Yes	Yes	No
	Derivation of the Equations of Motion	Simple	Hard	Moderate	Moderate	Moderate
	Order of Nonlinearity	Moderate	High	Moderate	Moderate	Moderate
	Matrices	Sparse	Dense	Moderately Dense	Moderately Dense	Dense
	Constant Mass Matrices	Yes	No	No	No	No
	Computation of System Energy	Req. Addit. Calc.*	Intrinsic	Intrinsic	Intrinsic	Intrinsic
	Computation of Reaction Forces	Intrinsic	Req. Addit. Calc.*	Req. Addit. Calc.*	Req. Addit. Calc.*	Req. Addit. Calc.*
	Physical Interpretation	Easy	Difficult	Difficult	Difficult	Difficult
	Stabilization	Required	Not Required	Required	Required	Not Required
Modeling	Modeling Systematization	Easy	Difficult	Difficult	Difficult	Difficult
	Analysis of Complex Systems	Easy	Difficult	Moderate	Moderate	Moderate
	Development of a General-Purpose Program	Easy	Difficult	Difficult	Difficult	Difficult
Computational Performance	Computational Efficiency	Moderately Efficient	Very Efficient	Efficient	Efficient	Efficient
	Required Time Step	Moderately High	High	Moderately High	Moderately Low	Low
	Accuracy	Accurate	Very accurate	Accurate	Accurate	Accurate

* Req. Addit. Calc. - Required Additional Calculation

8. Concluding remarks

In this work, a comparative analysis of several distinct approaches for modeling and analysis of closed loop kinematic chains using the Lagrangian formulation has been presented. For that, the classical Newton-Euler and Lagrangian methods were revisited. Subsequently, the three approaches based on the Lagrangian formulations were described with the main goal of examining their similarities and highlighting their differences, when compared with the Newton-Euler and the Lagrangian methods. The three approaches investigated were the cut joint approach, the clearance joint constraint model, and the elastic joint formulation. In the sequel of this process, the academic slider-crank mechanism was utilized as a demonstrative application example, which allowed to quantify the peculiarities of each approach considered. In a simple manner, the three formulations proposed were aimed at transforming the closed loop topology of the slider-crank mechanism and, eventually, to facilitate the application of the Lagrangian formulation to obtain the equations of motion for each approach. This allows for alternative ways compared to the traditional mathematical and computational efforts required in the derivative process, when the Lagrangian formulation is applied to multibody systems having closed loop kinematic chains.

The dynamic response of the slider-crank mechanism multibody model with all the five different formulations described (Newton-Euler, Lagrangian, Lagrangian with cut joint, Lagrangian with clearance joint, and Lagrangian with elastic joint), together with their computational accuracy and efficiency were analyzed and compared. From the main results obtained with computational simulations, it can be stated that the Lagrangian formulations with cut joints, clearance joints, and elastic joints are all effective and attractive to model and analyze multibody systems with closed loop structures. In addition, based on the results obtained and discussed in this study, none of the formulations can be identified to be superior to the others, since there are several features that affect their performance, as observed in the critical analysis summarized in Table 6. The cut joint approach allows mimicking the motion of an ideal mechanical system, although it requires two additional constraint equations which result in a set of DAE and lower computational efficiency. On the other hand, the clearance joint method only introduces one additional constraint, which might present numerical difficulties, when the clearance size is too small. Lastly, the elastic joint approach is based on a set of ODE, since it does not involve any kinematic constraint, and the closure of the system's loop is done through a force constraint, requiring a proper selection of the stiffness value to control both the joint eccentricity and computational efficiency.

Finally, this work can be expanded to implement the described approaches to more complex systems, and to incorporate other features, such as contact forces that can be generated in the clearance joints, damping elements to smooth the oscillatory behavior related to the elastic joint formulation, etc. A detailed analysis of alternative numerical integration schemes, methods to handle the violation of constraints, can also be potential further developments.

Acknowledgments

This work has been supported by Portuguese Foundation for Science and Technology, under the national support to R&D units grant, with the reference project UIDB/04436/2020 and UIDP/04436/2020, as well as through IDMEC, under LAETA, project UIDB/50022/2020.

References

1. I. Newton, Philosophiae Naturalis Principia Mathematica. London (1687).
2. L. Euler, Nova methodus motum corporum rigidorum determinandi. The Euler Archive, E-479 (1776).
3. J.L. Lagrange, Mécanique Analytique. L'Académie Royal des Sciences, 1st ed. Courcier, Paris (1788).
4. B. Paul, Analytical dynamics of mechanisms - a computer oriented overview. Mechanism and Machine Theory, 10(6) (1975) 481-507.
5. N. Orlandea, M.A. Chase, D.A. Calahan, A Sparsity-Oriented Approach to the Dynamic Analysis and Design of Mechanical Systems - Part 1. Journal of Engineering for Industry, 99(3) (1977) 773-779.
6. N. Orlandea, M.A. Chase, D.A. Calahan, A Sparsity-Oriented Approach to the Dynamic Analysis and Design of Mechanical Systems - Part 2. Journal of Engineering for Industry, 99(3) (1977) 780-784.

7. B. Dasgupta, T.S. Mruthyunjaya, A Newton-Euler formulation for the inverse dynamics of the Stewart platform manipulator. Mechanism and Machine Theory, 33(8) (1998) 1135-1152.
8. D.I.M. Forehand, R. Khanin, M.P. Cartmell, A Lagrangian multibody code for deriving the symbolic state-space equations of motion for open-loop systems containing flexible beams. Math. Comput. Simulat., 67(1-2) (2004) 85-98.
9. E. Stoneking, Newton-Euler dynamic equations of motion for a multi-body spacecraft. Collection of Technical Papers - AIAA Guidance, Navigation, and Control Conference 2007, 2, (2007) 1368-1380.
10. E. Paraskevopoulos, N. Potosakis, S. Natsiavas, An augmented Lagrangian formulation for the equations of motion of multibody systems subject to equality constraints. Procedia Engineering, 199 (2017) 747-752.
11. d'Alembert, J., Traité de Dynamique. Paris (1743).
12. W.R. Hamilton, On a General Method in Dynamics. Philosophical Transactions of the Royal Society, Part II (1834) 247-308.
13. G.A. Maggi, Principii della Teoria Matematica del Movimento dei Corpi: Corso di Meccanica Razionale, Ed. Ulrico Hoepli, Milano (1896).
14. J.W. Gibbs, On the fundamental formulae of dynamics. American Journal of Mathematics, 2(1) (1879) 49-64.
15. P. Appell, Sur les mouvements de roulment; equations du mouvement analougues a celles de lagrange. Comptes Rendus, 129 (1899) 317-320.
16. P.E.B., Jourdain, Note on an analogue at Gauss' principle of least constraint. Quarterly Journal on Pure Applied Mathematics, 40 (1909) 153-197.
17. T.R. Kane, Dynamics of nonholonomic systems. Journal of Applied Mechanics, 28(4) (1961) 574-578.
18. T.R. Kane, C.F. Wang, On the Derivation of Equations of Motion. Journal of the Society for Industrial and Applied Mechanics, 13(2) (1965) 482-487.
19. T.R. Kane, D.A., Levinson, Formulation of Equation of Motion for Complex Spacecraft. Journal of Guidance and Control, 3(2) (1980) 99-112.
20. P.A.M. Dirac, Lectures on Quantum Mechanics. Yeshiva Univ., New York, NY (1964).
21. W. Hooker, G. Margulies, The dynamical attitude equations for n-body satellite. J. Astronaut. Sci. 12 (1965) 123-128.
22. L.A. Pars, A Treatise on Analytical Dynamics. Oxbow Press, Woodridge, CT (1979).
23. F.E. Udwadia, R.E. Kalaba, A new perspective on constrained motion. Proc. R. Soc. London Ser. A Math. Phys. Sci. 439(1906) (1992) 407-410.
24. M. Borri, C. Bottasso, P. Mantegazza, Equivalence of Kane's and Maggi's equations. Meccanica, 25 (1990) 272-274.
25. J.G. Papastavridis, Maggi's equations of motion and the determination of constraint reactions. Journal of Guidance and Control, 13(2) (1990) 213-220.
26. A.H. Bajodah, D.H. Hodges, Y.-H. Chen, Nonminimal generalized Kane's impulse-momentum relations Journal of Guidance and Control, 27(6) (2004) 1088-1092.
27. G. Vossoughi, H. Pendar, Z. Heidari, S. Mohammadi, Assisted passive snake-like robots: Conception and dynamic modeling using Gibbs-Appell method. Robotica, 26(3) (2008) 267-276.
28. N.V. Khang, Kronecker product and a new matrix form of Lagrangian equations with multipliers for constrained multibody systems. Mech. Res. Commun., 38(4) (2011) 294-299.
29. E.T. Stoneking, Implementation of Kane's method for a spacecraft composed of multiple rigid bodies. AIAA Guidance, Navigation, and Control (GNC) Conference, (2013) 2013-4649.
30. K. Chadaj, P. Malczyk, J. Fraczek, A parallel Hamiltonian formulation for forward dynamics of closed-loop multibody systems. Multibody System Dynamic, 39 (2017) 39-51.
31. A. Talaeizadeh, M. Forootan, M. Zabihi, H.N. Pishkenari, Comparison of Kane's and Lagrange's Methods in Analysis of Constrained Dynamical Systems. Robotica, 38(12) (2020) 2138-2150.
32. W. Schiehlen, (ed.) Multibody Systems Handbook. Springer, Berlin (1990).
33. P.E. Nikravesh, Some Methods for Dynamic Analysis of Constrained Mechanical Systems: A Survey. NATO ASI Series, Series F: Computer and Systems Sciences, 9 (1984) 351-368.
34. W. Schiehlen, Multibody System Dynamics: Roots and Perspectives. Multibody System Dynamics, 1(2) (1997) 149-188.
35. P.E. Nikravesh, H.A. Affifi, Construction of the Equations of Motion for Multibody Dynamics Using Point and Joint Coordinates. In Computer-Aided Analysis of Rigid and Flexible Mechanical Systems. Vol. 268 of NATO ASI Series E: Applied Sciences (1994) 31-60.
36. P.E. Nikravesh, G. Gim, Systematic Construction of the Equations of Motion for Multibody Systems Containing Closed Kinematic Loop. Journal of Mechanical Design, 115 (1993) 143-149.
37. J.J. McPhee, S.M. Redmond, Modelling multibody systems with indirect coordinates. Computer Methods in Applied Mechanics and Engineering, 195(50-51) (2006) 6942-6957.
38. J.G. Jalón, Twenty-five years of natural coordinates. Multibody System Dynamics, 18 (2007) 15-33.
39. C.M. Pappalardo, A natural absolute coordinate formulation for the kinematic and dynamic analysis of rigid multibody systems. Nonlinear Dynamics, 81(4) (2015) 1841-1869.
40. K. Luo, H. Hu, C. Liu, Q. Tian, Model order reduction for dynamic simulation of a flexible multibody system via absolute nodal coordinate formulation. Comput. Methods Appl. Mech. Engrg., 324 (2017) 573-594.
41. C.M. Pappalardo, D. Guida, Dynamic analysis of planar rigid multibody systems modeled using natural absolute coordinates. Applied and Computational Mechanics, 12 (2018) 73-110.

42. L.P. Quinto, S.B. Gonçalves, M.T. Silva, Design of a passive exoskeleton to support sit-to-stand movement: A 2D model for the dynamic analysis of motion. Biosystems and Biorobotics, 22 (2019) 299-303.
43. X.M. Xu, J.H. Luo, X.G. Feng, H.J. Peng, Z.G. Wu, A generalized inertia representation for rigid multibody systems in terms of natural coordinates. Mechanism and Machine Theory, 157 (2020) 104174.
44. A. Angeli, W. Desmet, F. Naets, Deep learning for model order reduction of multibody systems to minimal coordinates. Computer Methods in Applied Mechanics and Engineering, 373 (2021) 113517.
45. E. Pennestrí, L. Vita, Strategies for the numerical integration of DAE systems in multibody dynamics. Comput. Appl. Eng. Educ., 12(2) (2004) 106-116.
46. P. Joli, N. Séguy, Z.-Q. Feng, A modular modeling approach to simulate interactively multibody systems with Baumgarte/Uzawa formulation. Journal of Nonlinear and Computational Dynamics, 3(1) (2008) 011011.
47. P.E. Nikravesh, Newtonian-based methodologies in multi-body dynamics. Journal of Multi-Body Dynamics, 222 (2008) 277-288.
48. M. Hiller, A. Kecskeméthy, Dynamics of Multibody Systems with Minimal Coordinates. In Computer-Aided Analysis of Rigid and Flexible Mechanical Systems. Vol. 268 of NATO ASI Series E: Applied Sciences (1994) 61-100.
49. S.K. Saha, W.O. Schiehlen, Recursive Kinematics and Dynamics for Parallel Structured Closed-Loop Multibody Systems. Mechanics of Structures and Machines, 29(2) (2001) 143-175.
50. J. Wang, C.M. Gosselin, L. Cheng, Modeling and simulation of robotic systems with closed kinematic chains using the virtual spring approach. Multibody System Dynamics, 7(2) (2002) 145-170.
51. P. Flores, H.M. Lankarani, Contact Force Models for Multibody Dynamics. Springer, (2016).
52. P.E. Nikravesh, An overview of several formulations for multibody dynamics. Product Engineering, Eco-Design, Technology and Green Energy, D. Talaba and T. Roche (Eds.), Springer, (2005) 189-226.
53. P.E. Nikravesh, Planar Multibody Dynamics: Formulation, Programming with MATLAB®, and Applications. Second Edition, CRC Press, Boca Raton (2019).
54. P.E. Nikravesh, Computer-Aided Analysis of Mechanical Systems. Prentice Hall, Engewood Cliffes (1988).
55. D.T. Greenwood, Principles of Dynamics, 2nd edn. Prentice Hall, Englewood Cliffs (1988).
56. E.J. Haug, Computer Aided Kinematics and Dynamics of Mechanical Systems Vol. 1: Basic Methods, Allyn Bacon, Boston (1989).
57. S.A. Emam, Generalized Lagrange's equations for systems with generalized constraints and distributed parameters. Multibody System Dynamics, 49 (2020) 95-117.
58. M. Arnold, DAE Aspects of Multibody System Dynamics. Surveys in Differential-Algebraic Equations, A. Ilchamann and T. Reis (Eds.), Springer, (2017) 41-106.
59. D. Pogorelov, Differential-algebraic equations in multibody system modeling. Numerical Algorithms, 19 (1998) 183-194.
60. L.F. Shampine, M.K. Gordon, Computer Solution of Ordinary Differential Equations, The Initial Value Problem, Freeman, San Francisco, CA (1975).
61. E. Eich-Soellner, C. Fuher, Numerical Methods in Multibody Dynamics. Vol. 45, Springer, Berlin (1998).
62. J. Baumgarte, Stabilization of constraints and integrals of motion in dynamical systems. Computer Methods in Applied Mechanics and Engineering, 1 (1972) 1-16.
63. R.A. Wehage, E.J. Haug, Generalized coordinate partitioning for dimension reduction in analysis of constrained systems. Journal of Mechanical Design, 104 (1982) 247-255.
64. C.O. Chang, P.E. Nikravesh, An adaptive constraint violation stabilization method for dynamic analysis of mechanical systems. Journal of Mechanisms, Transmissions, and Automation in Design, 107 (1985) 488-492.
65. E. Bayo, J.G. Jalón, M.A. Serna, A modified Lagrangian formulation for the dynamic analysis of constrained mechanical systems. Comput. Methods Appl. Math. 71(2) (1988) 183-195.
66. J.K. Kim, I.S. Chung, B.H. Lee, Determination of the Feedback Coefficients for the Constraint Violation Stabilization Method. Proceedings of the Institution of Mechanical Engineers, Part C: Journal of Mechanical Engineering Science, 204 (1990) 233-242.
67. S. Yoon, R.M. Howe, D.T. Greenwood, Constraint violation stabilization using gradient feedback in constrained dynamics simulation. Journal of Guidance, Control, and Dynamics, 15(6) (1992) 1467-1474.
68. J.C. Chiou, S.D. Wu, Constraint violation stabilization using input-output feedback linearization in multibody dynamic analysis. Journal of Guidance, Control, and Dynamics, 21(2) (1998) 222-228.
69. Q. Yu, I.M. Chen, A direct violation correction method in numerical simulation of constrained multibody systems. Computational Mechanics, 26(1) (2000) 52-57.
70. Z. Weijia, P. Zhenkuan, W. Yibing, An automatic constraint violation stabilization method for differential/algebraic equations on multibody system dynamics. Applied Mathematics and Mechanics, 21(1) (2000) 103-108.
71. W. Blajer, Methods for constraint violation suppression in the numerical simulation of constrained multibody systems - a comparative study. Computational Methods in Applied Mathematics, 200(13-16) (2011) 1568-1576.
72. M.A. Neto, J. Ambrósio, Stabilization methods for the integration of DAE in the presence of redundant constraints. Multibody System Dynamics, 10 (2003) 81-105.
73. D.J. Braun, M. Goldfarb, Eliminating constraint drift in the numerical simulation of constrained dynamical systems. Computational Methods in Applied Mathematics, 198(37-40) (2009) 3151-3160.
74. P. Flores, M. Machado, E. Seabra, M.T. Silva, A parametric study on the Baumgarte stabilization method for forward dynamics of constrained multibody systems. Journal of Computational and Nonlinear Dynamics, 6(1) (2011) 0110191.
75. J. Zhang, D. Liu, Y. Liu, A constraint violation suppressing formulation for spatial multibody dynamics with singular mass matrix. Multibody System Dynamics, 36(1) (2016) 87-110.

76. F. Marques, A.P. Souto, P. Flores, On the constraints violation in forward dynamics of multibody systems. Multibody System Dynamics, 39 (2017) 385-419.
77. C.M. Pappalardo, A. Lettieri, D. Guida, Stability analysis of rigid multibody mechanical systems with holonomic and nonholonomic constraints. Archive of Applied Mechanics, 90 (2020) 1961-2005.
78. A.W., Pila, Introduction To Lagrangian Dynamics, Springer (2020).
79. J.G. Jalón, E. Bayo, Kinematic and Dynamics Simulations of Multibody Systems: The Real-Time Challenge. Springer, New York (1994).
80. K.A. Atkinson, An Introduction to Numerical Analysis, 2nd edn. Wiley, New York (1989).
81. V.B. Ho, On the Principle of Least Action. International Journal of Physics, 6(2) (2018) 47-52.
82. Q. Tian, P. Flores, H.M. Lankarani, A comprehensive survey of the analytical, numerical and experimental methodologies for dynamics of multibody mechanical systems with clearance or imperfect joints. Mechanism and Machine Theory, 122 (2018) 1-57.
83. P.E. Nikravesh, Systematic reduction of multibody equations of motion to a minimal set. International Journal of Non-Linear Mechanics, 25(2-3) (1990) 143-151.
84. M.S. Pereira, P. Nikravesh, Impact Dynamics of Multibody Systems with Frictional Contact Using Joint Coordinates and Canonical Equations of Motion. Nonlinear Dynamics, 9 (1996) 53-71.
85. T. Yoshikawa, K. Hosoda, Modeling of flexible manipulator using virtual links and passive joints. International Journal of Robotics Research, 15(3) (1996) 290-299.
86. J. Ambrósio, P. Verissimo, Improved bushing models for general multibody systems and vehicle dynamics. Multibody System Dynamics, 22 (2009) 341-365.
87. J. Costa, J. Peixoto, P. Moreira, A.P. Souto, P. Flores, H.M. Lankarani, H.M. Influence of the Hip Joint Modeling Approaches on the Kinematics of Human Gait. Journal of Tribology, 138(3) (2016) 031201.
88. S. Erkaya, S. Doğan, E. Şefkatlıoğlu, Analysis of the joint clearance effects on a compliant spatial mechanism. Mechanism and Machine Theory, 104 (2016) 255-273.
89. F. Marques, F. Isaac, N. Dourado, A.P. Souto, P. Flores, H.M. Lankarani, A Study on the Dynamics of Spatial Mechanisms with Frictional Spherical Clearance Joints. Journal of Computational and Nonlinear Dynamics, 12(5) (2017) 051013.
90. F. Marques, F. Isaac, N. Dourado, P. Flores, An enhanced formulation to model spatial revolute joints with radial and axial clearances. Mechanism and Machine Theory, 116 (2017) 123-144.
91. F. Isaac, F. Marques, N. Dourado, P. Flores, A finite element model of a 3D dry revolute joint incorporated in a multibody dynamic analysis. Multibody System Dynamics, 45(3) (2019) 293-313.
92. S. Erkaya, Determining power consumption using neural model in multibody systems with clearance and flexible joints. Multibody System Dynamics, 47(2) (2019) 165-181.
93. J. Alves, N. Peixinho, M.T. Da Silva, P. Flores, H.M. Lankarani, A comparative study of the viscoelastic constitutive models for frictionless contact interfaces in solids. Mechanism and Machine Theory, 85 (2015) 172-188.
94. L. Skrinjar, J. Slavič, M. Boltežar, A review of continuous contact-force models in multibody dynamics. International Journal of Mechanical Sciences, 145 (2018) 171-187.
95. J. Zhang, W. Li, L. Zhao, G. He, A continuous contact force model for impact analysis in multibody dynamics. Mechanism and Machine Theory, 153 (2020) 103946.
96. E. Pennestrì, V. Rossi, P. Salvini, P.P. Valentini, Review and comparison of dry friction force models. Nonlinear Dynamics, 83(4) (2016) 1785-1801.
97. F. Marques, P. Flores, J.C.P. Claro, H.M. Lankarani, Modeling and analysis of friction including rolling effects in multibody dynamics: a review. Multibody System Dynamics, 45(2) (2019) 223-244.
98. M. Qian, Z. Qin, S. Yan, L. Zhang, A comprehensive method for the contact detection of a translational clearance joint and dynamic response after its application in a crank-slider mechanism. Mechanism and Machine Theory, 145 (2020) 103717.
99. N. Potosakis, E. Paraskevopoulos, S. Natsiavas, Application of an augmented Lagrangian approach to multibody systems with equality motion constraints. Nonlinear Dynamics, 99(1) (2020) 753-776.
100. J. Beckers, T. Verstraten, B. Verrelst, F. Contino, J. Van Mierlo, Analysis of the dynamics of a slider-crank mechanism locally actuated with an act-and-wait controller. Mechanism and Machine Theory, 159 (2021) 104253.
101. S. Zarkandi, A novel optimization-based method to find multiple solutions for path synthesis of planar four-bar and slider-crank mechanisms. Proceedings of the Institution of Mechanical Engineers, Part C: Journal of Mechanical Engineering Science (2021) https://doi.org/10.1177/0954406220983369
102. J.M. Veciana Fontanet, L. Jordi Nebot, E. Lores Garcia, Residual vibration reduction in back-and-forth moving systems driven by slider-crank mechanisms working through a dead point configuration. Mechanism and Machine Theory, 158 (2021) 104239.
103. X. Wu, Y. Sun, Y. Wang, Y. Chen, Correlation dimension and bifurcation analysis for the planar slider-crank mechanism with multiple clearance joints. Multibody System Dynamics (2021) https://doi.org/10.1007/s11044-020-09769-3

Appendix A. Constraint equations for the slider-crank mechanism

In order to obtain the kinematic constraint equations for the slider-crank mechanism, it is necessary to develop the kinematic loops associated with the joints. Figure A.1 shows three possible kinematic chains for the slider-crank mechanism's joints, which are not scaled drawn.

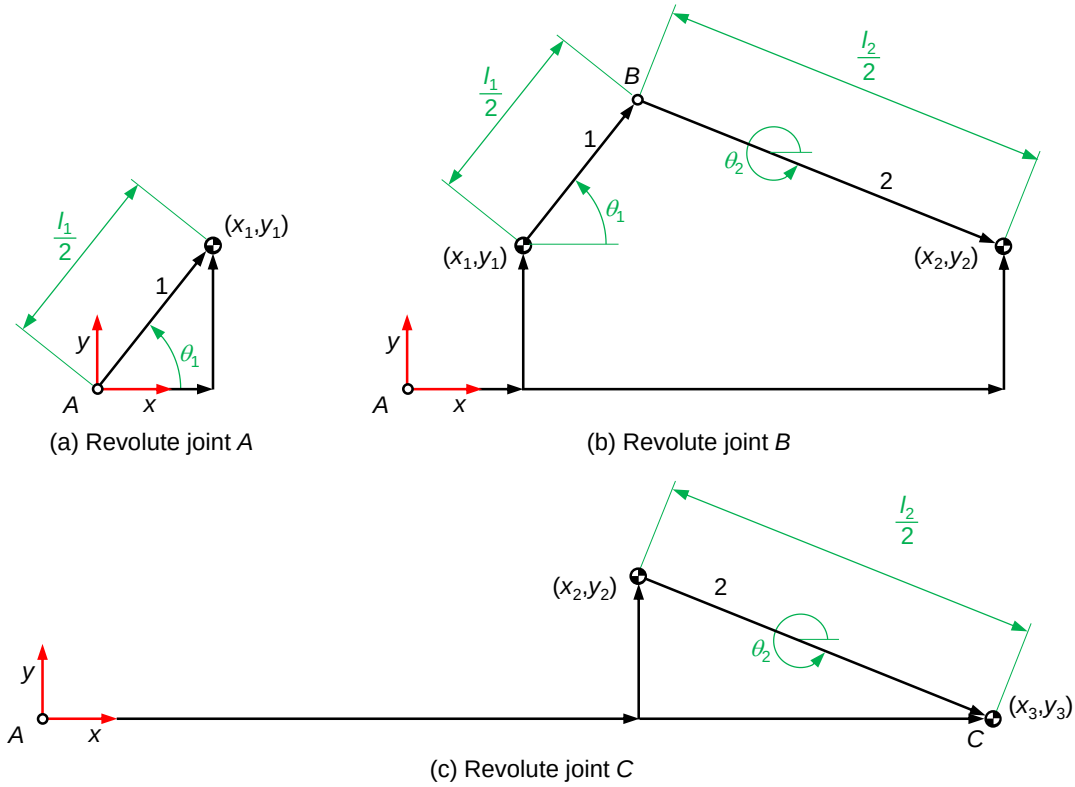

Fig. A.1. Closed kinematic chains for the revolute joints of the slider-crank mechanism.

In what follows, three absolute coordinates are utilized to obtain the kinematic constraint equations, namely two Cartesian coordinates associated with the center of mass of each body and one angular coordinate related to the orientation of the slider-crank mechanism's bodies. Thus, the revolute joint *A* imposes two restrictions, which can be materialized by two algebraic constraints expressed as

$$\Phi_1 \equiv x_1 - \frac{l_1}{2}\cos\theta_1 = 0 \tag{A.1}$$

$$\Phi_2 \equiv y_1 - \frac{l_1}{2}\sin\theta_1 = 0 \tag{A.2}$$

In a similar manner, the remaining revolute joints *B* and *C* can be formulated with regard to the corresponding kinematic loops represented in Fig. A.1, yielding

$$\Phi_3 \equiv x_1 + \frac{l_1}{2}\cos\theta_1 - x_2 + \frac{l_2}{2}\cos\theta_2 = 0 \tag{A.3}$$

$$\Phi_4 \equiv y_1 + \frac{l_1}{2}\sin\theta_1 - y_2 + \frac{l_2}{2}\sin\theta_2 = 0 \tag{A.4}$$

$$\Phi_5 \equiv x_2 + \frac{l_2}{2}\cos\theta_2 - x_3 = 0 \tag{A.5}$$

$$\Phi_6 \equiv y_2 + \frac{l_2}{2}\sin\theta_2 - y_3 = 0 \tag{A.6}$$

The translational joint can be modeled by a set of two simple kinematic constraints as

$$\Phi_7 \equiv y_3 = 0 \tag{A.7}$$

$$\Phi_8 \equiv \theta_3 = 0 \tag{A.8}$$

The eight kinematic scleronomic holonomic constraints can be written in a compact form as

$$\mathbf{\Phi} \equiv \mathbf{\Phi}(\mathbf{c}) = \mathbf{0} \tag{A.9}$$

where **c** represents the array of absolute coordinates given by Eq. (1). In the most general case, position constraints given by Eq. (A.9) are nonlinear algebraic equations.

The constraint equations at the velocity level can be obtained as the first time derivative of the position constraints (A.1)-(A.8), yielding

$$\dot{\Phi}_1 \equiv \dot{x}_1 + \frac{l_1}{2}\sin\theta_1\dot{\theta}_1 = 0 \tag{A.10}$$

$$\dot{\Phi}_2 \equiv \dot{y}_1 - \frac{l_1}{2}\cos\theta_1\dot{\theta}_1 = 0 \tag{A.11}$$

$$\dot{\Phi}_3 \equiv \dot{x}_1 - \frac{l_1}{2}\sin\theta_1\dot{\theta}_1 - \dot{x}_2 - \frac{l_2}{2}\sin\theta_2\dot{\theta}_2 = 0 \tag{A.12}$$

$$\dot{\Phi}_4 \equiv \dot{y}_1 + \frac{l_1}{2}\cos\theta_1\dot{\theta}_1 - \dot{y}_2 + \frac{l_2}{2}\cos\theta_2\dot{\theta}_2 = 0 \tag{A.13}$$

$$\dot{\Phi}_5 \equiv \dot{x}_2 - \frac{l_2}{2}\sin\theta_2\dot{\theta}_2 - \dot{x}_3 = 0 \tag{A.14}$$

$$\dot{\Phi}_6 \equiv \dot{y}_2 + \frac{l_2}{2}\cos\theta_2\dot{\theta}_2 - \dot{y}_3 = 0 \tag{A.15}$$

$$\dot{\Phi}_7 \equiv \dot{y}_3 = 0 \tag{A.16}$$

$$\dot{\Phi}_8 \equiv \dot{\theta}_3 = 0 \tag{A.17}$$

The velocity constraints equations (A.10)-(A.17) can be written in a matrix structure as

$$\begin{bmatrix} 1 & 0 & \frac{l_1}{2}\sin\theta_1 & 0 & 0 & 0 & 0 & 0 & 0 \\ 0 & 1 & -\frac{l_1}{2}\cos\theta_1 & 0 & 0 & 0 & 0 & 0 & 0 \\ 1 & 0 & -\frac{l_1}{2}\sin\theta_1 & -1 & 0 & -\frac{l_2}{2}\sin\theta_2 & 0 & 0 & 0 \\ 0 & 1 & \frac{l_1}{2}\cos\theta_1 & 0 & -1 & \frac{l_2}{2}\cos\theta_2 & 0 & 0 & 0 \\ 0 & 0 & 0 & 1 & 0 & -\frac{l_2}{2}\sin\theta_2 & -1 & 0 & 0 \\ 0 & 0 & 0 & 0 & 1 & \frac{l_2}{2}\cos\theta_2 & 0 & -1 & 0 \\ 0 & 0 & 0 & 0 & 0 & 0 & 0 & 1 & 0 \\ 0 & 0 & 0 & 0 & 0 & 0 & 0 & 0 & 1 \end{bmatrix} \begin{Bmatrix} \dot{x}_1 \\ \dot{y}_1 \\ \dot{\theta}_1 \\ \dot{x}_2 \\ \dot{y}_2 \\ \dot{\theta}_2 \\ \dot{x}_3 \\ \dot{y}_3 \\ \dot{\theta}_3 \end{Bmatrix} = \begin{Bmatrix} 0 \\ 0 \\ 0 \\ 0 \\ 0 \\ 0 \\ 0 \\ 0 \\ 0 \end{Bmatrix} \tag{A.18}$$

or in a compact form as

$$\dot{\mathbf{\Phi}} \equiv \mathbf{D}\dot{\mathbf{c}} = \mathbf{0} \tag{A.19}$$

where **D** represents the Jacobian matrix, that is, the matrix of the partial derivatives, $\partial\mathbf{\Phi}/\partial\mathbf{c}$, and $\dot{\mathbf{c}}$ is the array of velocities given by Eq. (27). It must be noticed that velocity constraints given by (A.19) are algebraic equations linear in velocities.

The time derivative of the velocity constraints yields the kinematic constraints at the acceleration level. Thus, the time derivative of velocity constraints (A.10)-(A.17) results in

$$\ddot{\Phi}_1 \equiv \ddot{x}_1 + \frac{l_1}{2}\sin\theta_1\ddot{\theta}_1 + \frac{l_1}{2}\cos\theta_1\dot{\theta}_1^2 = 0 \tag{A.20}$$

$$\ddot{\Phi}_2 \equiv \ddot{y}_1 - \frac{l_1}{2}\cos\theta_1\ddot{\theta}_1 + \frac{l_1}{2}\sin\theta_1\dot{\theta}_1^2 = 0 \tag{A.21}$$

$$\ddot{\Phi}_3 \equiv \ddot{x}_1 - \frac{l_1}{2}\sin\theta_1\ddot{\theta}_1 - \frac{l_1}{2}\cos\theta_1\dot{\theta}_1^2 - \ddot{x}_2 - \frac{l_2}{2}\sin\theta_2\ddot{\theta}_2 - \frac{l_2}{2}\cos\theta_2\dot{\theta}_2^2 = 0 \tag{A.22}$$

$$\ddot{\Phi}_4 \equiv \ddot{y}_1 + \frac{l_1}{2}\cos\theta_1\ddot{\theta}_1 - \frac{l_1}{2}\sin\theta_1\dot{\theta}_1^2 - \ddot{y}_2 + \frac{l_2}{2}\cos\theta_2\ddot{\theta}_2 - \frac{l_2}{2}\sin\theta_2\dot{\theta}_2^2 = 0 \tag{A.23}$$

$$\ddot{\Phi}_5 \equiv \ddot{x}_2 - \frac{l_2}{2}\sin\theta_2\ddot{\theta}_2 - \frac{l_2}{2}\cos\theta_2\dot{\theta}_2^2 - \ddot{x}_3 = 0 \tag{A.24}$$

$$\ddot{\Phi}_6 \equiv \ddot{y}_2 + \frac{l_2}{2}\cos\theta_2\ddot{\theta}_2 - \frac{l_2}{2}\sin\theta_2\dot{\theta}_2^2 - \ddot{y}_3 = 0 \tag{A.25}$$

$$\ddot{\Phi}_7 \equiv \ddot{y}_3 = 0 \tag{A.26}$$

$$\ddot{\Phi}_8 \equiv \ddot{\theta}_3 = 0 \tag{A.27}$$

In a similar manner to the velocity constraints, the acceleration constraints (A.20)-(A.27) can be written in a matrix structure as

$$\begin{bmatrix}
1 & 0 & \frac{l_1}{2}\sin\theta_1 & 0 & 0 & 0 & 0 & 0 & 0 \\
0 & 1 & -\frac{l_1}{2}\cos\theta_1 & 0 & 0 & 0 & 0 & 0 & 0 \\
1 & 0 & -\frac{l_1}{2}\sin\theta_1 & -1 & 0 & -\frac{l_2}{2}\sin\theta_2 & 0 & 0 & 0 \\
0 & 1 & \frac{l_1}{2}\cos\theta_1 & 0 & -1 & \frac{l_2}{2}\cos\theta_2 & 0 & 0 & 0 \\
0 & 0 & 0 & 1 & 0 & -\frac{l_2}{2}\sin\theta_2 & -1 & 0 & 0 \\
0 & 0 & 0 & 0 & 1 & \frac{l_2}{2}\cos\theta_2 & 0 & -1 & 0 \\
0 & 0 & 0 & 0 & 0 & 0 & 0 & 1 & 0 \\
0 & 0 & 0 & 0 & 0 & 0 & 0 & 0 & 1
\end{bmatrix}
\begin{Bmatrix}
\ddot{x}_1 \\ \ddot{y}_1 \\ \ddot{\theta}_1 \\ \ddot{x}_2 \\ \ddot{y}_2 \\ \ddot{\theta}_2 \\ \ddot{x}_3 \\ \ddot{y}_3 \\ \ddot{\theta}_3
\end{Bmatrix}
=
\begin{Bmatrix}
-\frac{l_1}{2}\cos\theta_1\dot{\theta}_1^2 \\
-\frac{l_1}{2}\sin\theta_1\dot{\theta}_1^2 \\
\frac{l_1}{2}\cos\theta_1\dot{\theta}_1^2 + \frac{l_2}{2}\cos\theta_2\dot{\theta}_2^2 \\
\frac{l_1}{2}\sin\theta_1\dot{\theta}_1^2 + \frac{l_2}{2}\sin\theta_2\dot{\theta}_2^2 \\
\frac{l_2}{2}\cos\theta_2\dot{\theta}_2^2 \\
\frac{l_2}{2}\sin\theta_2\dot{\theta}_2^2 \\
0 \\ 0
\end{Bmatrix} \tag{A.28}$$

or in a compact form as

$$\ddot{\mathbf{\Phi}} \equiv \mathbf{D}\ddot{\mathbf{c}} = \boldsymbol{\gamma} \tag{A.29}$$

where $\mathbf{D}$ represents the Jacobian matrix, $\ddot{\mathbf{c}}$ denotes the array of accelerations given by Eq. (14), and $\boldsymbol{\gamma}$ is the right-hand side vector of acceleration constraints that contains the quadratic terms in velocities. Finally, it is worth noting that acceleration constraints given by (A.29) are algebraic equations linear in accelerations.

Appendix B. Joint reaction forces expressed as $\mathbf{D}^{\mathrm{T}}\boldsymbol{\lambda}$

The joint reaction forces are usually written as function of Jacobian matrix and Lagrange multipliers (30). This relation can be demonstrated using the d'Alembert's principle of zero virtual work, that is, the forces associated with ideal constraints do not produce work. This principle was first stated by Lagrange [3], reason why it is often called Lagrange-d'Alembert's principle [57].

With the purpose to proof Eq. (30), let consider the most general form of the holonomic constraint equations for constrained multibody systems written as [53]

$$\boldsymbol{\Phi} \equiv \boldsymbol{\Phi}(\mathbf{c}, t) = \mathbf{0} \tag{B.1}$$

which restrict the system's motion in the configuration space constituted by coordinates $\mathbf{c}$.

The virtual displacement of the system configuration, which is an imaginary variation of the kinematic configuration of the systems at a stationary instant of time, is consistent with the constraints enforced on the system's motion [79]. It is worth recalling that a virtual quantity or variation, δ, acts in a similar way as an operator with respect to independent variables only, since the virtual variables are assumed to be fixed during a virtual displacement. It was Lagrange's choice symbol δ to emphasize the virtual character of the variation. Actually, δ is not related to differentiation, but it is associated with the concept of virtual displacement only. The variation of the constraint equations (B.1) is, by definition, be expressed as

$$\delta\boldsymbol{\Phi} = \frac{\partial \boldsymbol{\Phi}}{\partial \mathbf{c}}\delta\mathbf{c} + \frac{\partial \boldsymbol{\Phi}}{\partial t}\delta t \tag{B.2}$$

in which the last term can be neglected, because the time is frozen for any virtual displacement, and, consequently, Eq. (B.2) can be simplified as

$$\delta\boldsymbol{\Phi} = \frac{\partial \boldsymbol{\Phi}}{\partial \mathbf{c}}\delta\mathbf{c} \Rightarrow \delta\boldsymbol{\Phi} = \mathbf{D}\delta\mathbf{c} \tag{B.3}$$

where $\mathbf{D}$ is the well-known Jacobian matrix, which contains the derivatives of the constraint equations with respect to the vector of coordinates $\mathbf{c}$, and $\delta\mathbf{c}$ represents the vector of virtual displacements of system's coordinates.

The analysis of Eq. (B.3) reveals that the constraints gradient, $\partial\boldsymbol{\Phi}/\partial\mathbf{c}$, is orthogonal to the virtual displacements, $\delta\mathbf{c}$, in the $\mathbf{c}$-configuration space constituted by all the coordinates, as it is shown in Fig. B.1. In other words, it can be said the $\delta\mathbf{c}$ adheres to constraint equations (B.1), in the measure that $\delta\mathbf{c}$ is perpendicular to the gradient of $\boldsymbol{\Phi}$ with respect to $\mathbf{c}$.

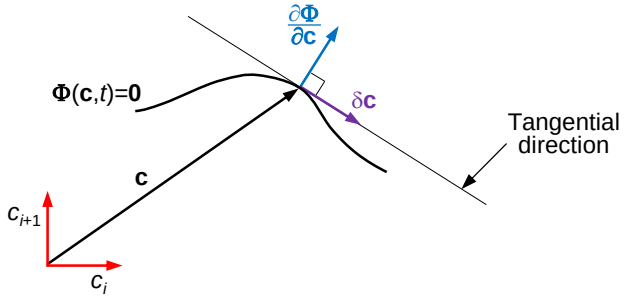

Fig. B.1. Admissible variations $\delta\mathbf{c}$ for constraint surface in the $\mathbf{c}$-configuration space.

Backing to Eq. (30), it is clear that the Lagrange multipliers vector, $\boldsymbol{\lambda}$, represents the array of joint reaction forces. Thus, according to the d'Alembert's principle, the virtual work done by the constraint forces can be written in the form

$$\delta U = \boldsymbol{\lambda}^{\mathrm{T}}\delta\boldsymbol{\Phi} = 0 \tag{B.4}$$

Introducing Eq. (B.3) into Eq. (B.4) yields

$$\boldsymbol{\lambda}^{\mathrm{T}}\mathbf{D}\delta\mathbf{c}=0 \tag{B.5}$$

Taking advantage of the following transpose of matrix product property from Algebra

$$(\mathbf{AB})^{\mathrm{T}}=\mathbf{B}^{\mathrm{T}}\mathbf{A}^{\mathrm{T}} \tag{B.6}$$

then, Eq. (B.5) can be rewritten as

$$(\mathbf{D}^{\mathrm{T}}\boldsymbol{\lambda})^{\mathrm{T}}\delta\mathbf{c}=0 \tag{B.7}$$

Finally, comparing Eqs. (30) and (B.7), it can be concluded that

$$\mathbf{h}_{\mathrm{r}}=\mathbf{D}^{\mathrm{T}}\boldsymbol{\lambda} \tag{B.8}$$

Appendix C. Lagrangian formulation for the slider-crank mechanism

The development of the Lagrange's equations of motion for the slider-crank mechanism presented in Fig. 1 is straightforward, resulting in a second order nonlinear differential equation in θ_1 (85). Thus, this appendix deals with the detailed derivation of those equations of motion based on the Lagrange's method. Since the slider-crank mechanism has one degree-of-freedom, the vectors of generalized coordinates and velocities can be established as

$$q=\{\theta_1\} \tag{C.1}$$

$$\dot{q}=\{\dot{\theta}_1\} \tag{C.2}$$

From the geometric analysis of the slider-crank system configuration, a constraint condition can be defined as

$$l_1\sin\theta_1=-l_2\sin\theta_2 \tag{C.3}$$

which leads to

$$\theta_2=\sin^{-1}\left(-\frac{l_1}{l_2}\sin\theta_1\right) \tag{C.4}$$

The first time derivative of Eq. (C.4) results in

$$\dot{\theta}_2=-\frac{l_1\cos\theta_1\dot{\theta}_1}{\sqrt{l_2^2-l_1^2\sin^2\theta_1}} \tag{C.5}$$

In order to obtain the Lagrange's equations of motion, it is first necessary to express the bodies' center of mass position in terms of generalized coordinate θ_1. With regard to Fig. 1b, the position of the center of mass of the crank can be written as

$$x_1=\frac{l_1}{2}\cos\theta_1 \tag{C.6}$$

$$y_1=\frac{l_1}{2}\sin\theta_1 \tag{C.7}$$

The velocity components of the center of mass of the crank, expressed in terms of the generalized coordinate and its time derivative, can be obtained by simple differentiating Eqs. (C.6) and (C.7), yielding

$$\dot{x}_1=-\frac{l_1}{2}\sin\theta_1\dot{\theta}_1 \tag{C.8}$$

$$\dot{y}_1 = \frac{l_1}{2}\cos\theta_1\dot{\theta}_1 \tag{C.9}$$

The kinetic and potential energies associated with crank can be established as

$$T_1 = \frac{1}{2}I_1\dot{\theta}_1^2 + \frac{1}{2}m_1\left(\dot{x}_1^2 + \dot{y}_1^2\right) = \frac{1}{2}I_1\dot{\theta}_1^2 + \frac{1}{8}m_1 l_1^2\dot{\theta}_1^2 \tag{C.10}$$

$$V_1 = m_1 g y_1 = \frac{1}{2}m_1 g l_1 \sin\theta_1 \tag{C.11}$$

In a similar manner, the position of the center of mass of the connecting rod can be written as

$$x_2 = l_1\cos\theta_1 + \frac{l_2}{2}\cos\theta_2 \tag{C.12}$$

$$y_2 = \frac{l_1}{2}\sin\theta_1 \tag{C.13}$$

The time derivatives of Eqs. (C.12) and (C.13) can be expressed as

$$\dot{x}_2 = -l_1\sin\theta_1\dot{\theta}_1 - \frac{l_2}{2}\sin\theta_2\dot{\theta}_2 \tag{C.14}$$

$$\dot{y}_2 = \frac{l_1}{2}\cos\theta_1\dot{\theta}_1 \tag{C.15}$$

Taking advantage of the Pythagorean identity together with Eqs. (C.3) and (C.5), the kinetic and potential energies associated with connecting rod can be established as

$$T_2 = \frac{1}{2}I_2\dot{\theta}_2^2 + \frac{1}{2}m_2\left(\dot{x}_2^2 + \dot{y}_2^2\right) = \frac{1}{2}I_2 l_1^2 A\dot{\theta}_1^2 + \frac{1}{2}m_2\left(l_1^2 B + \frac{l_1^4}{4}C + l_1^3 D + \frac{l_1^2}{4}E\right)\dot{\theta}_1^2 \tag{C.16}$$

$$V_2 = m_2 g y_2 = \frac{1}{2}m_2 g l_1 \sin\theta_1 \tag{C.17}$$

where *A*, *B*, *C*, *D* and *E* terms are established as

$$A = \frac{\cos^2\theta_1}{l_2^2 - l_1^2\sin^2\theta_1} \tag{C.18}$$

$$B = \sin^2\theta_1 \tag{C.19}$$

$$C = \frac{\sin^2\theta_1\cos^2\theta_1}{l_2^2 - l_1^2\sin^2\theta_1} \tag{C.20}$$

$$D = \frac{\sin^2\theta_1\cos\theta_1}{\sqrt{l_2^2 - l_1^2\sin^2\theta_1}} \tag{C.21}$$

$$E = \cos^2\theta_1 \tag{C.22}$$

Similarly, the position of the center of mass of the slider can be written as

$$x_3 = l_1\cos\theta_1 + l_2\cos\theta_2 \tag{C.23}$$

$$y_3 = 0 \tag{C.24}$$

The time derivatives of Eqs. (C.23) and (C.24) can be expressed as follows

$$\dot{x}_3 = -l_1 \sin\theta_1 \dot{\theta}_1 - l_2 \sin\theta_2 \dot{\theta}_2 \tag{C.25}$$

$$\dot{y}_3 = 0 \tag{C.26}$$

Once again, taking advantage of the Pythagorean identity together with Eqs. (C.3) and (C.5), the kinetic and potential energies associated with the slider can be defined as

$$T_3 = \frac{1}{2} m_3 \left(\dot{x}_3^2 + \dot{y}_3^2 \right) = \frac{1}{2} m_3 \left(l_1^2 B + l_1^4 C + 2 l_1^3 D \right) \dot{\theta}_1^2 \tag{C.27}$$

$$V_3 = 0 \tag{C.28}$$

where *B*, *C*, and *D* terms have been defined previously.

The Lagrangian function for the slider-crank mechanism shown in Fig. 1, which is the core to derive the Lagrange's equations of motion, can be established as

$$L = T_1 + T_2 + T_3 - V_1 - V_2 - V_3 \tag{C.29}$$

Introducing the corresponding equations presented above into Eq. (C.29), yields

$$\begin{aligned} L = {} & \frac{1}{2} I_1 \dot{\theta}_1^2 + \frac{1}{8} m_1 l_1^2 \dot{\theta}_1^2 - \frac{1}{2} m_1 g l_1 \sin\theta_1 + \\ & \frac{1}{2} I_2 l_1^2 A \dot{\theta}_1^2 + \frac{1}{2} m_2 \left(l_1^2 B + \frac{l_1^4}{4} C + l_1^3 D + \frac{l_1^2}{4} E \right) \dot{\theta}_1^2 - \frac{1}{2} m_2 g l_1 \sin\theta_1 + \\ & \frac{1}{2} m_3 \left(l_1^2 B + l_1^4 C + 2 l_1^3 D \right) \dot{\theta}_1^2 \end{aligned} \tag{C.30}$$

The derivatives of the Lagrangian function required to obtain the Lagrange's equations of motion of the slider-crank mechanism can be expressed as

$$\frac{\partial L}{\partial \dot{\theta}_1} = I_1 \dot{\theta}_1 + \frac{1}{4} m_1 l_1^2 \dot{\theta}_1 + I_2 l_1^2 A \dot{\theta}_1 + m_2 \left(l_1^2 B + \frac{l_1^4}{4} C + l_1^3 D + \frac{l_1^2}{4} E \right) \dot{\theta}_1 + m_3 \left(l_1^2 B + l_1^4 C + 2 l_1^3 D \right) \dot{\theta}_1 \tag{C.31}$$

$$\begin{aligned} \frac{\mathrm{d}}{\mathrm{d}t} \left(\frac{\partial L}{\partial \dot{\theta}_1} \right) = {} & I_1 \ddot{\theta}_1 + \frac{1}{4} m_1 l_1^2 \ddot{\theta}_1 + \\ & I_2 l_1^2 A \ddot{\theta}_1 + m_2 \left(l_1^2 B + \frac{l_1^4}{4} C + l_1^3 D + \frac{l_1^2}{4} E \right) \ddot{\theta}_1 + m_3 \left(l_1^2 B + l_1^4 C + 2 l_1^3 D \right) \ddot{\theta}_1 + \\ & I_2 l_1^2 \dot{A} \dot{\theta}_1 + m_2 \left(l_1^2 \dot{B} + \frac{l_1^4}{4} \dot{C} + l_1^3 \dot{D} + \frac{l_1^2}{4} \dot{E} \right) \dot{\theta}_1 + m_3 \left(l_1^2 \dot{B} + l_1^4 \dot{C} + 2 l_1^3 \dot{D} \right) \dot{\theta}_1 \end{aligned} \tag{C.32}$$

$$\begin{aligned} \frac{\partial L}{\partial \theta_1} = {} & -\frac{1}{2} m_1 g l_1 \cos\theta_1 + \frac{1}{2} I_2 l_1^2 A' \dot{\theta}_1^2 + \frac{1}{2} m_2 \left(l_1^2 B' + \frac{l_1^4}{4} C' + l_1^3 D' + \frac{l_1^2}{4} E' \right) \dot{\theta}_1^2 - \\ & \frac{1}{2} m_2 g l_1 \cos\theta_1 + \frac{1}{2} m_3 \left(l_1^2 B' + l_1^4 C' + 2 l_1^3 D' \right) \dot{\theta}_1^2 \end{aligned} \tag{C.33}$$

where

$$\dot{A} = A' \dot{\theta}_1 \tag{C.34}$$

$$\dot{B} = B' \dot{\theta}_1 \tag{C.35}$$

$$\dot{C} = C' \dot{\theta}_1 \tag{C.36}$$

$$\dot{D} = D' \dot{\theta}_1 \tag{C.37}$$

$$\dot{E} = E'\dot{\theta}_1 \tag{C.38}$$

$$A' = -\frac{\sin 2\theta_1 \left(l_2^2 - l_1^2\right)}{\left(l_2^2 - l_1^2 \sin^2\theta_1\right)^2} \tag{C.39}$$

$$B' = \sin 2\theta_1 \tag{C.40}$$

$$C' = \frac{2\sin\theta_1 \cos^3\theta_1}{l_2^2 - l_1^2 \sin^2\theta_1} - \frac{2\sin^3\theta_1 \cos\theta_1 \left(l_2^2 - l_1^2\right)}{\left(l_2^2 - l_1^2 \sin^2\theta_1\right)^2} \tag{C.41}$$

$$D' = \frac{2\sin\theta_1 \cos^2\theta_1 - \sin^3\theta_1}{\sqrt{l_2^2 - l_1^2 \sin^2\theta_1}} + \frac{\sin^3\theta_1 \cos^2\theta_1 l_1^2}{\left(l_2^2 - l_1^2 \sin^2\theta_1\right)^{\frac{3}{2}}} \tag{C.42}$$

$$E' = -\sin 2\theta_1 \tag{C.43}$$

Finally, introducing Eqs. (C.32) and (C.33) into Eq. (57), and after mathematical treatment, the Lagrange's equations of motion for the slider-crank mechanism can be written in the form

$$m\ddot{\theta}_1 = h \tag{C.44}$$

where the inertia and generalized force terms are expressed as

$$\begin{aligned} m = I_1 + I_2 \frac{l_1^2 \cos^2\theta_1}{l_2^2 - l_1^2 \sin^2\theta_1} + \frac{1}{4}\left(m_1 + m_2 \cos^2\theta_1\right) l_1^2 + \left(m_2 + m_3\right) l_1^2 \sin^2\theta_1 + \\ \left(\frac{1}{4} m_2 + m_3\right) \frac{l_1^4 \sin^2\theta_1 \cos^2\theta_1}{l_2^2 - l_1^2 \sin^2\theta_1} + \left(m_2 + 2m_3\right) \frac{l_1^3 \sin^2\theta_1 \cos\theta_1}{\sqrt{l_2^2 - l_1^2 \sin^2\theta_1}} \end{aligned} \tag{C.45}$$

$$\begin{aligned} h = \frac{1}{2} I_2 \frac{l_1^2 \sin 2\theta_1 \left(l_2^2 - l_1^2\right)}{\left(l_2^2 - l_1^2 \sin^2\theta_1\right)^2} \dot{\theta}_1^2 + \frac{1}{8} m_2 l_1^2 \sin 2\theta_1 \dot{\theta}_1^2 - \frac{1}{2}\left(m_2 + m_3\right) l_1^2 \sin 2\theta_1 \dot{\theta}_1^2 - \\ \frac{1}{8}\left(m_2 + 4m_3\right) l_1^4 \left(\frac{\sin 2\theta_1 \cos^2\theta_1}{l_2^2 - l_1^2 \sin^2\theta_1} - \frac{\sin 2\theta_1 \sin^2\theta_1 \left(l_2^2 - l_1^2\right)}{\left(l_2^2 - l_1^2 \sin^2\theta_1\right)^2} \right) \dot{\theta}_1^2 - \\ \frac{1}{2}\left(m_2 + 2m_3\right) l_1^3 \left(\frac{\sin 2\theta_1 \cos\theta_1 - \sin^3\theta_1}{\sqrt{l_2^2 - l_1^2 \sin^2\theta_1}} + \frac{\sin^3\theta_1 \cos^2\theta_1 l_1^2}{\left(l_2^2 - l_1^2 \sin^2\theta_1\right)^{\frac{3}{2}}} \right) \dot{\theta}_1^2 - \frac{1}{2}\left(m_1 + m_2\right) g l_1 \cos\theta_1 \end{aligned} \tag{C.46}$$